

MAS836 – Sensor Technologies for Interactive Environments

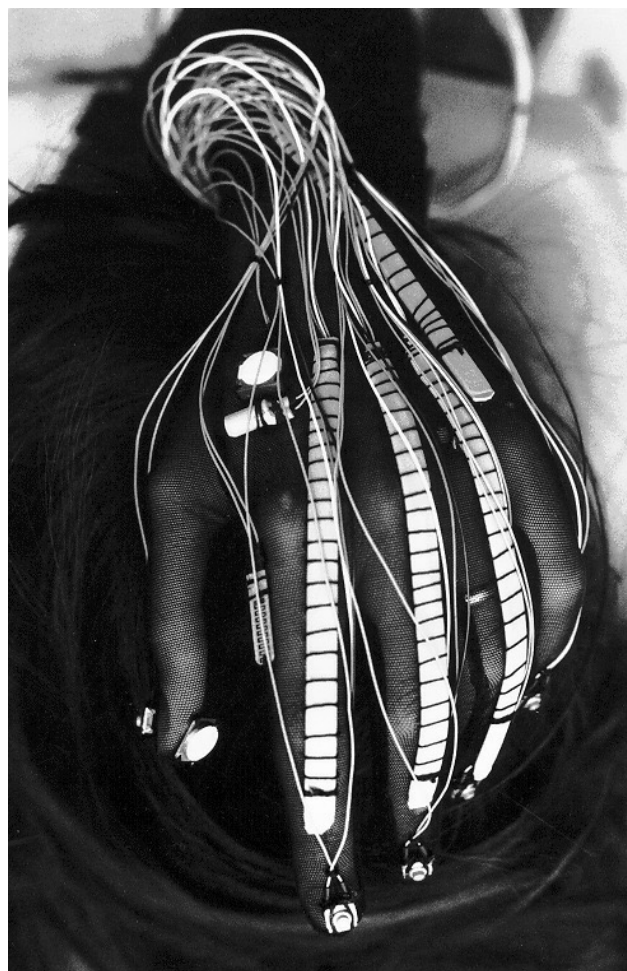


Lecture 5 – Pressure Sensors Pt. 2 and Piezoelectrics

Some FSR-Bendy-Sensor Gloves



*Mattel's Power Glove
1989*



*Laetitia Sonami's Lady's Glove
(STEIM, 1997)*



The 22-sensor CyberGlove has three flexion sensors per finger, four abduction sensors, a palm-arch sensor, and sensors to measure flexion and abduction. Each sensor is extremely thin and flexible being virtually undetectable in the lightweight elastic glove.

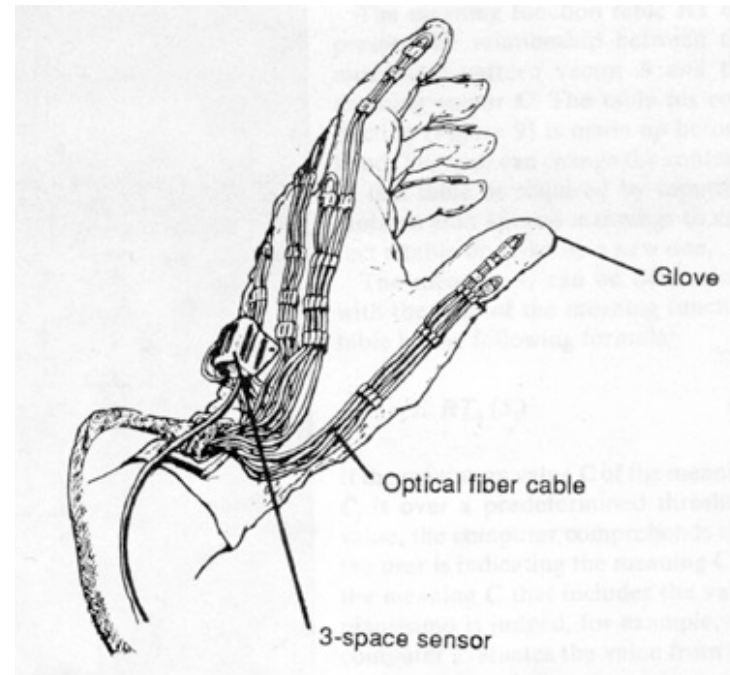
Immersion's Cyber Glove

Data Gloves



5DT Data Glove 16

Black stretch lycra
Minimum dynamic range is 8 bits.
Fiber optics based
14 Sensors in total
2 Sensors per finger. Abduction sensors between fingers.



- Abraded-cladding fiber optic bend sensor in the Data Glove

Data Glove by Tom Zimmerman (VPL)

U.S. Patent

Jun. 26, 1990

4,937,444

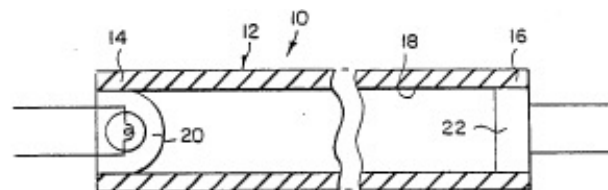
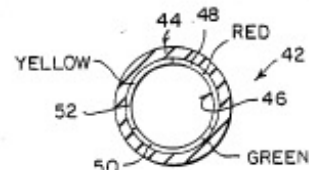
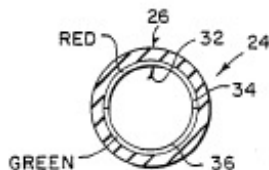
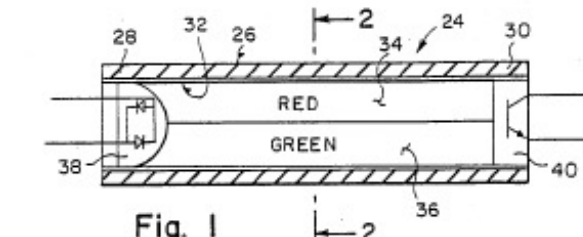
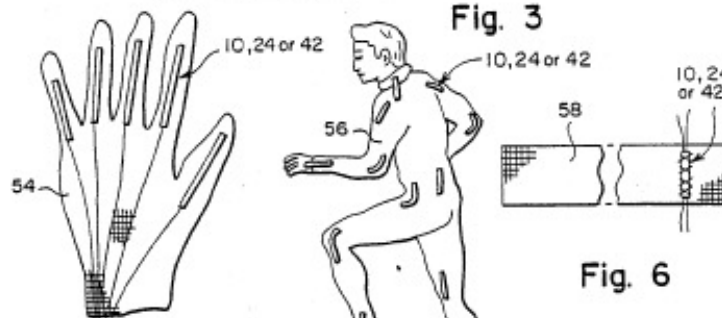


Fig. 3



10, 24 or 42

10, 24 or 42

10, 24 or 42

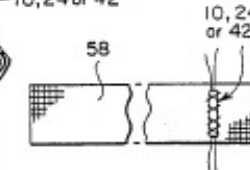
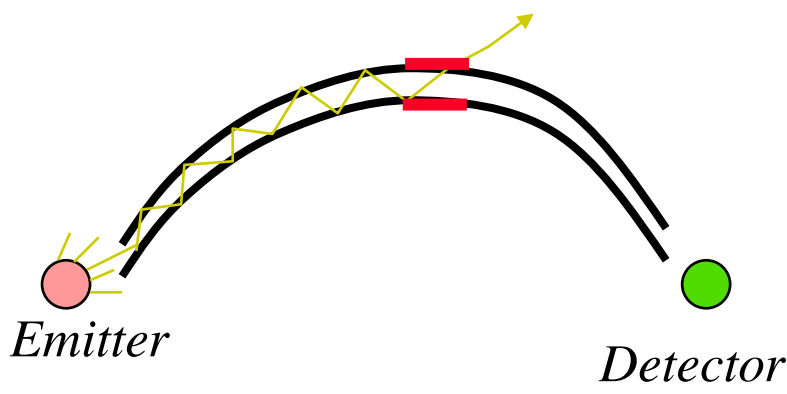


Fig. 6



- Cladding of a Graded Index Optical Fiber is abraded at point where sensitivity is desired
- When fiber bent, light leaks out as a function of bend angle
 - Drop in signal at detector
- Patented by Tom Zimmerman (lab alum) at VPL in 1985 & 1990.

Measurand's Shape Tape

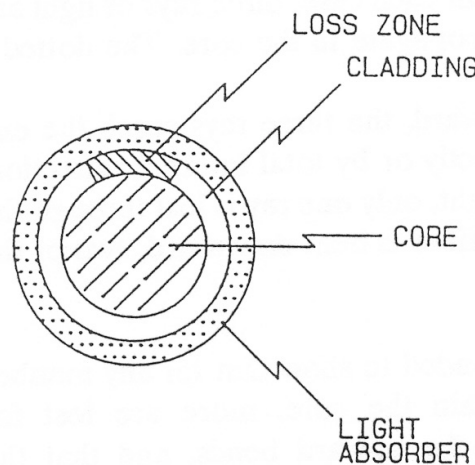
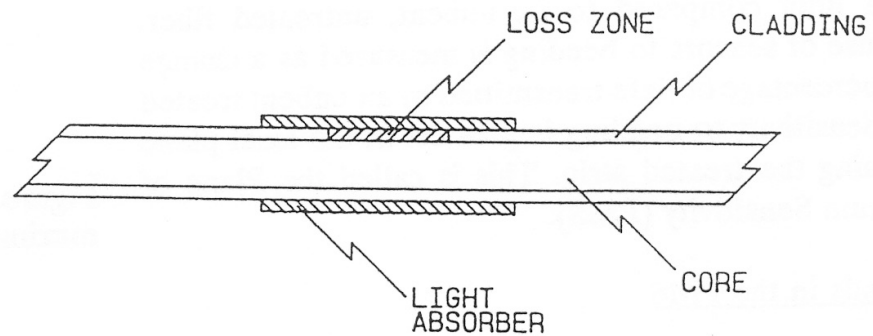
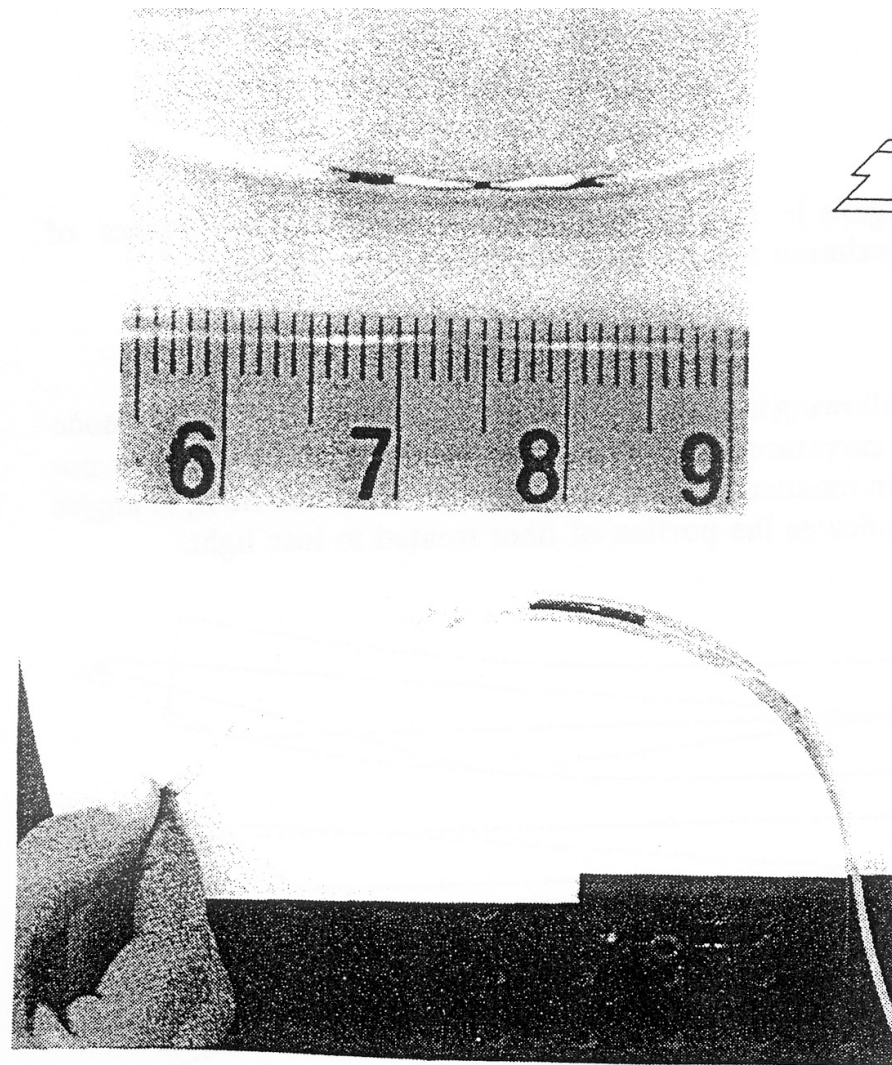
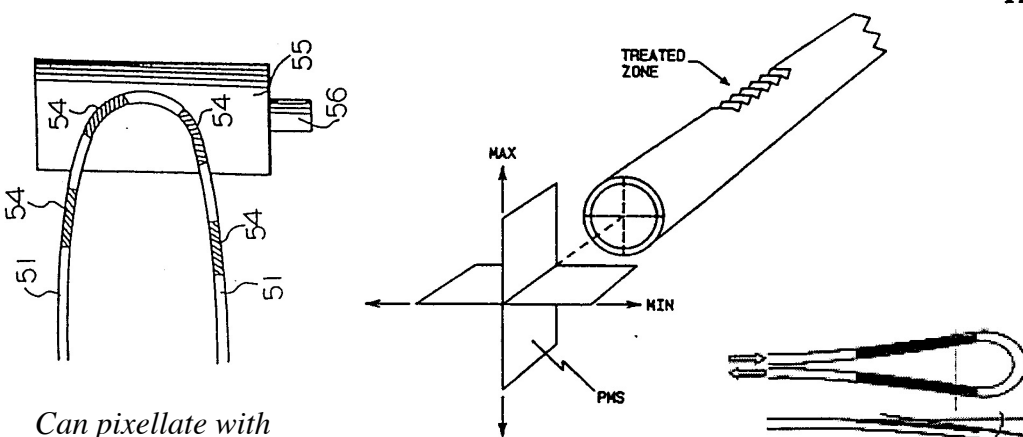


Figure 3: Examples of BEF sensors. Upper left: 200/230 micron BEF, coated with black epoxy over treated zone (scale marks: cm); Lower left: A BEF sensor attached to a thin metal substrate can be bent over large angles.; Right: construction of BEF sensor.

Measurand's Shape Tape



Can pixellate with an array of fibers, with treatment at different locations

The dotted line indicates the portion of fiber treated to lose light.

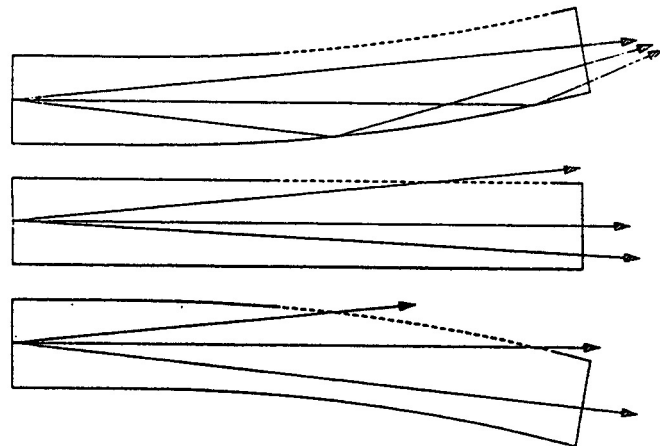
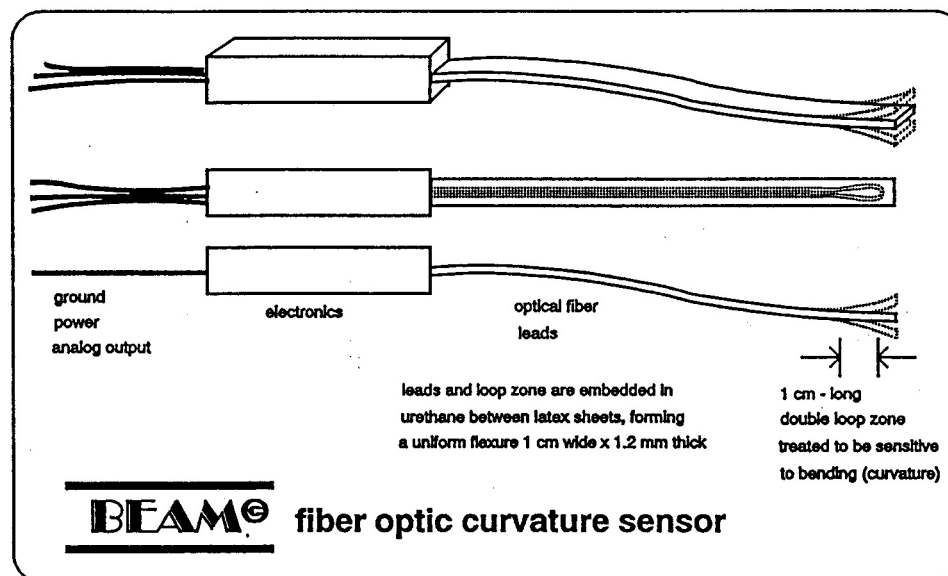
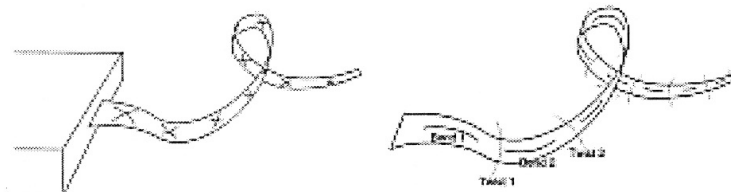


Figure 1: Plastic fiber with a treated strip. Planes of maximum and minimum sensitivity are indicated.

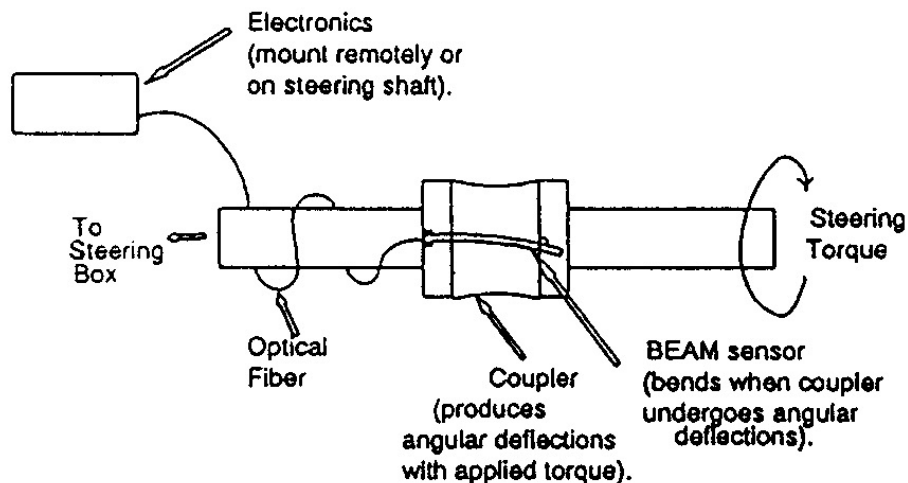


If the fiber is bent upward, the three rays reach the end of the fiber either directly or by total internal reflection. When the fiber is straight, only one ray is lost through the treated portion. If the fiber is bent downward, two of the rays are lost.

This model can be extended to show that for any number of rays contained within the core, more are lost for downward bends than for upward bends, and that the straight fiber represents an intermediate case. If all the cladding were removed, upward bends would be indistinguishable from downward bends, and the sensor would not be useful when straight, the most likely position for embedded fibers.



How ShapeTape Measures Twist



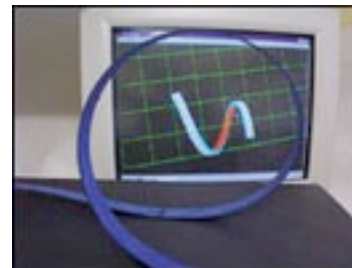
*Bend fibers near center of strip
Twist fibers near edges*

Can also wrap fibers around center?



SHAPE TAPE™ uses paired loops to sense twist and bend along a ribbon substrate. In this case, sums and differences correspond to twist and bend, and there is no control loop used in ordinary applications.

Shape Tape



Characteristics, S1280CS multiplexed ShapeTape™

(Specifications will vary for other lengths, number of sensors, etc.)

Dimensions of tape: 1.3 x 13 x 1800 mm nominal

Dimensions of interface box: 16 x 54 x 168 mm nominal

Operating temperature: -20 to 50 deg c

Sensitive zone: outboard 480 mm contains 16 sensors arranged in 8 pairs

Sensor length: each sensor integrates curvature over a 60 mm portion of the sensitive zone

Sensor pair: each pair resolves bend and twist, using calibration constants

Calibration: Circle, twist, & flat poses yield stored calibration constants

Data: x,y,z and orientation at 16 or more points along sensitive zone, relative to inboard reference end

Calibrated Range of each sensor: ± 40 mm radius bend; ± 22.8 deg twist

Safe Bending radius: ± 20 mm radius

Spatial sampling limits: each monotonic (single polarity) curve requires two sensor lengths

Operating range for end of 'U' shape: two elliptical volumes, 160 x 250 mm each.

Endpoint accuracy within operating range and sampling limits: 1-3% of length is a reasonable expectation for postional errors; thus, for the first 100 mm of a tape, the error can be expected to be 1-3 mm, and if the tape is 1000 mm long, the error at the tip can be expected to be 10-30 mm.

Endpoint resolution: 0.3 mm rms, x,y,or z; 0.5 deg, roll, pitch, or yaw

Other locations on tape: errors reduce toward inboard reference end, within range and sampling limits

Maximum data acquisition speed: 110 Hz

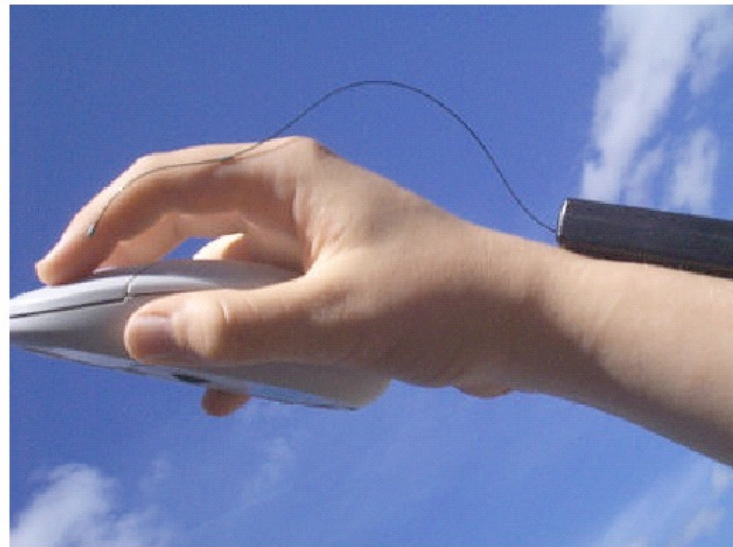
Included: Wall mount power supply (60 Hz, 120VAC), serial cable, interface box, and tape

http://www.youtube.com/v/ZMZr1jNDVGY&color1=0xb1b1b1&color2=0xcfcfcf&hl=en_US&feature=player_embedded&fs=1

Shape Tape Products

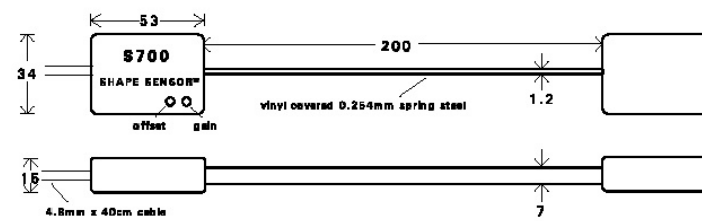
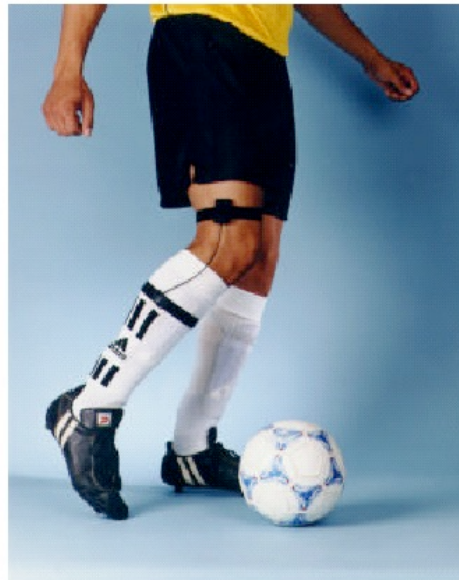
S720 MINIATURE JOINT ANGLE SHAPE SENSOR™

Revision 20020912



S700 JOINT ANGLE SHAPE SENSOR

Revision 20020912



(dimensions in millimeters unless otherwise indicated)



Shapewrap
the portable go anywhere motion capture system

Fiber Optic Pressure Sensors

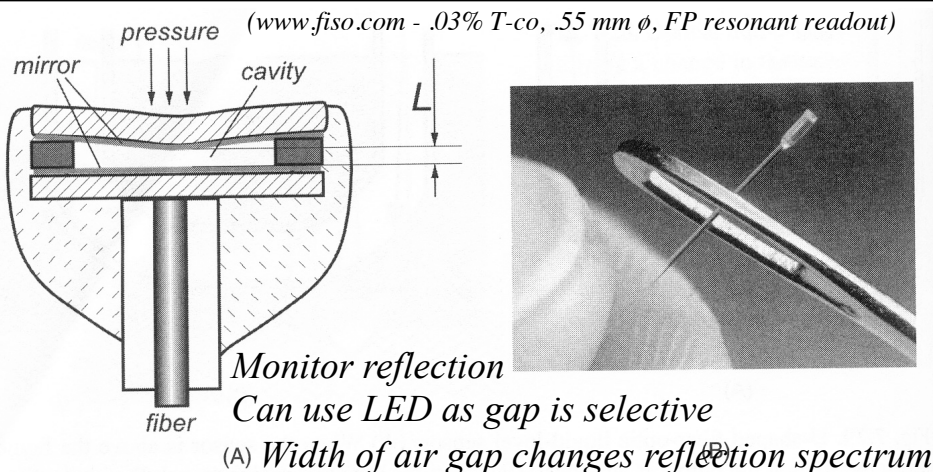


Fig. 7.31. Construction of a Fabry-Perot pressure sensor (A) and view of FISO FOP-M pressure sensor (B).

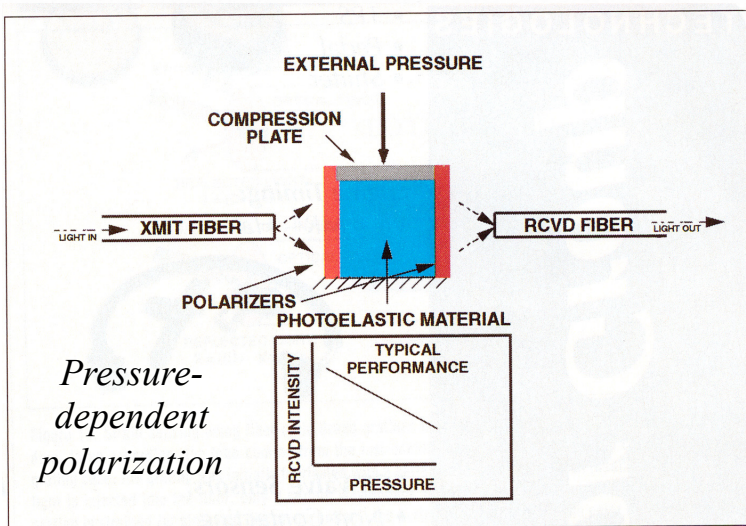


Figure 11. In an extrinsic fiber-optic pressure sensor based on polarization, pressure is applied to a plate that compresses a compliant photoelastic material. Polarized light is sent into the photoelastic material, which then rotates the polarization state of the light as the pressure changes. Another bulk polarizer (when used in this configuration it is called an analyzer) only transmits light of a certain polarization rotation. The sensor works in the following manner: with no pressure applied, there is no polarization rotation, hence the maximum field intensity emerges from the analyzer. As the pressure increases, more and more polarization rotation happens, resulting in decreasing intensity emerging from the analyzer.

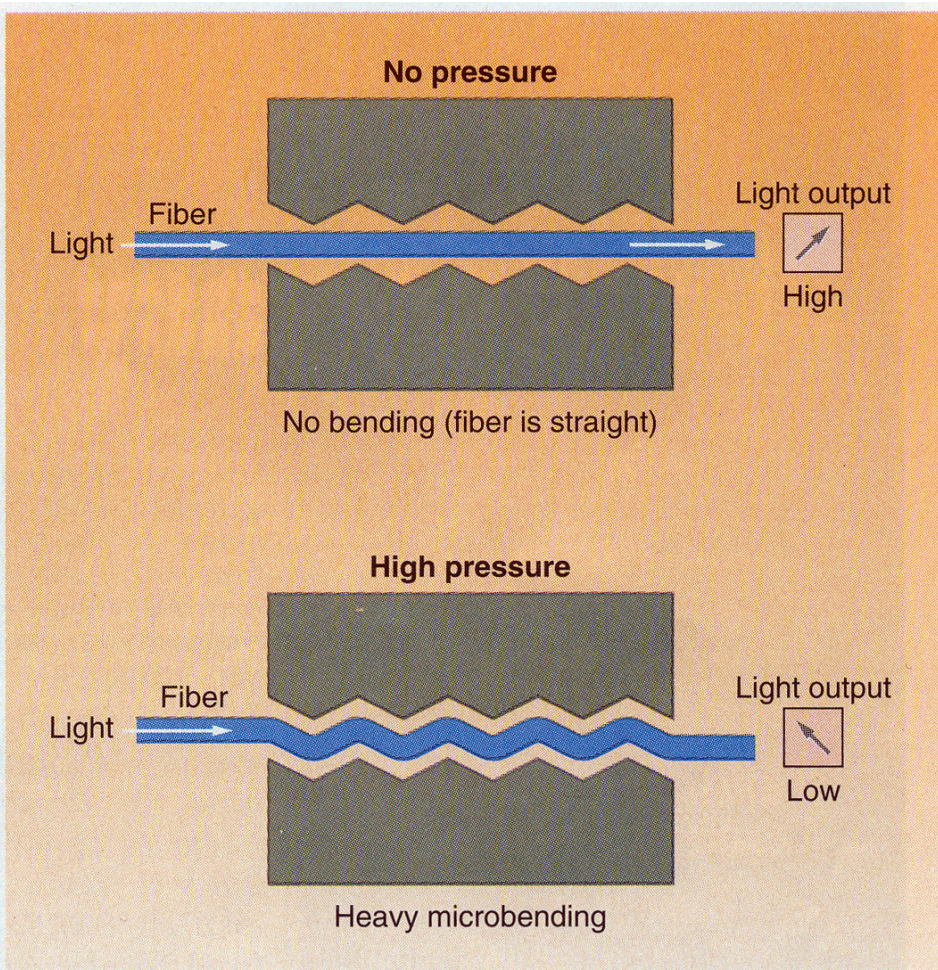
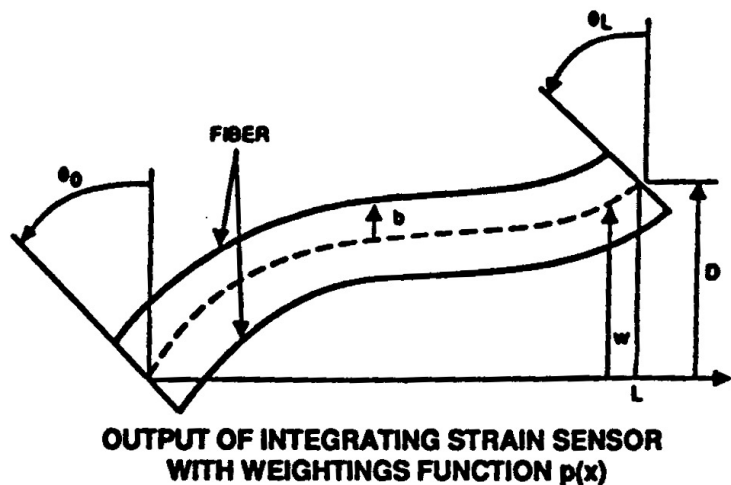


FIGURE 1. Fiber pressure sensor depends on microbending in a fiber mounted between two grooved plates. Increasing the pressure increases microbending losses, so pressure can be inferred from measurements of transmitted optical power.

AXIS - Alignment Transfer By Integrated Strain

P = sensor weighting (uniform)
b(x) = half diameter
w''(x) = rod curvature
x = distance along rod



$$-\Delta L = \epsilon = \int_0^L P b(x) w'(x) dx$$

$$= P b(x) w'(x) \Big|_0^L - P b'(x) w(x) \Big|_0^L + \int_0^L P b''(x) w(x) dx$$

If $b(x) = B$

$$\epsilon = P B [w(L) - w(0)] = P B (\theta_L - \theta_0) \text{ (ANGLE OUTPUT)}$$

If $b(x) = K(1 - x/L)$

$$S = -K P w'(0) + K P/L [w(L) - w(0)]$$

$$= -K P (\theta_0 - D/L) \text{ (DISPLACEMENT OUTPUT)}$$

Figure 1. AXIS Analysis.

- Invented by Len Wilk, Draper Lab
 - US Patent # 4,788,868 (1988)
- Output of a strain-measuring loop draped across a beam depends *only* on the difference between the angles of the ends

Three-Angle measurements with twist

Note: D must be fairly small to avoid snapping measuring fiber or wire

As shown in Figure 2, a pair of fibers in the (nominally) $y z$ plane will provide a measure of the relative rotation about the x axis (e.g. the pitch angle):

$$\Theta_p = \Delta L_y / D \quad (2)$$

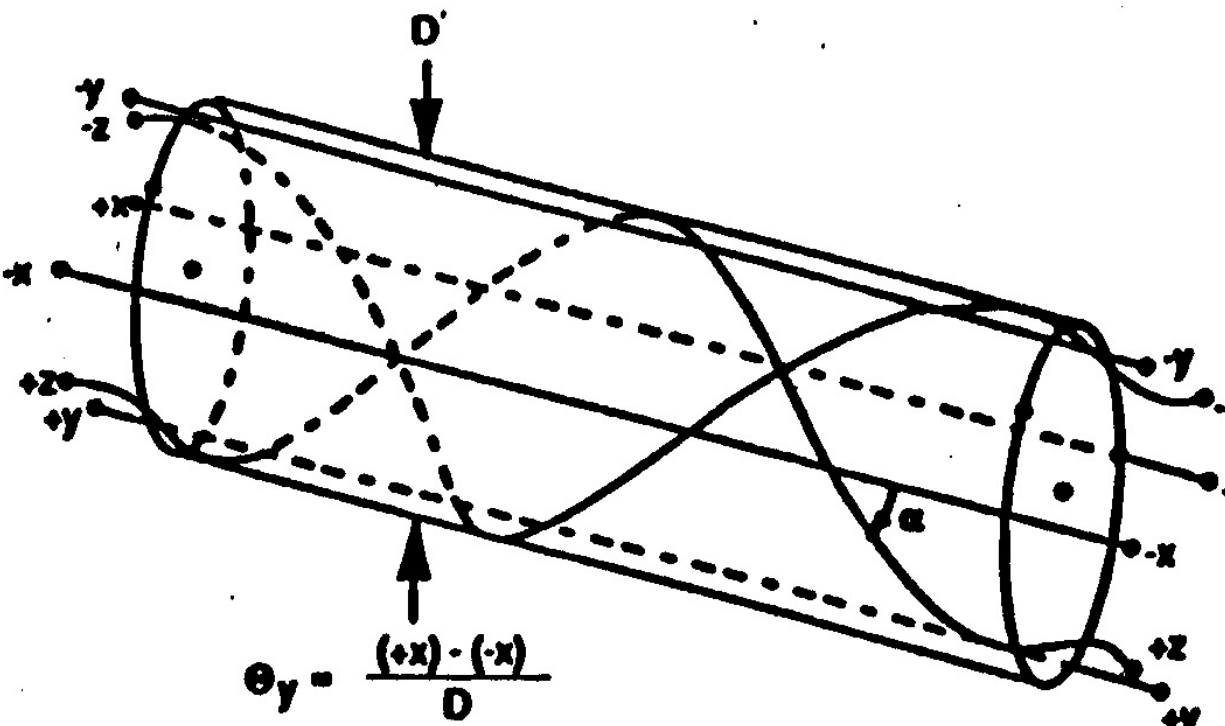
The pair of fibers in the (nominally) $x z$ plane provide the yaw angle,

$$\Theta_y = \Delta L_x / D \quad (3)$$

while a clockwise helical fiber compared to a counterclockwise helical fiber provides the roll (twist) angle,

$$\Theta_r = \Delta L_z \sin \alpha / D \quad (4)$$

where α is the helix angle, D is the diameter separating the pairs of fibers, and ΔL is the difference in length between the fibers of a pair.



$$\Theta_y = \frac{(+x) - (-x)}{D}$$

$$\Theta_p = \frac{(+y) - (-y)}{D}$$

$$\Theta_r = \frac{(+z) - (-z)}{D} \sin \alpha$$

- Helical windings provide measurement of twist



Some topological comments are in order. (1) The above configuration will provide the three angles independently given that the magnitude of the angles does not get too large (of order 30 degrees). (2) Bending and twisting that is constrained to one plane can be accommodated to large angles without topological limit. (3) Several rods can be joined in series: if the rods are joined at fixed right angles in cardinal directions, then the fiber pairs, rod to rod, can be joined so as to provide the proper angular transformations; if the rods are constrained to lie in cardinal planes, but at (fixed) arbitrary angles in these planes, and a double set of fibers implemented, the double pairs of fibers can be proportionally combined for proper transformations; with a triple set of fibers, the rods can be at any arbitrary fixed angles, and proportional combinations among the fiber pairs will provide the correct transformations.

Measurement of displacement with weighting

If the strain sensor has proportional weighting (i.e., the sensitivity diminishes uniformly from the left end to the right end, i.e., $p = K(1 - x/L)$, then the integrating strain sensor's output will be linearly related to the angle and the deflection D, regardless of the shape of the cable:

$$\epsilon = -KB w'(0) + \frac{KB}{L} (w(L) - w(0)) = -KB(\theta_0 + D/L) \quad (4)$$

Add another fiber loop with graded sensitivity to disambiguate displacement

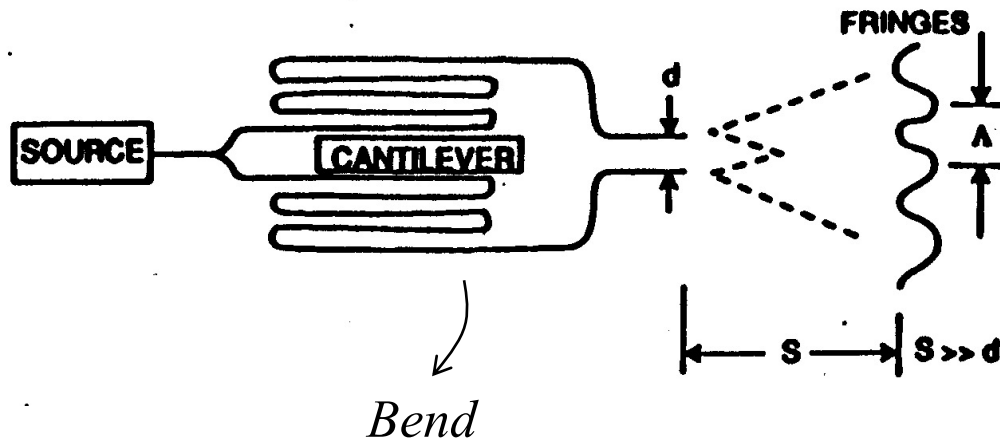
AXIS Interferometric Readout

Thus, we see that angle and displacement of two reference points can be measured by integrating strain sensors. In the case of an optical fiber, the optical phase shift as a function of strain is given by the photoelastic effect

$$\phi(\epsilon) = knL(1 + \epsilon) - \frac{kn^3L}{2} (\rho_{12} - v(\rho_{11} + \rho_{12}))\epsilon \quad (5)$$

where $k = 2\pi/\lambda$, n is the refractive index, v is Poisson's ratio, and ρ_{11} and ρ_{12} are the photoelastic constants. The cable would be instrumented with pairs of integrating strain sensors on opposite sides of the cable, operating in a differential mode.

Single-Axis Interferometer Schematic



Results in an arcsecond of deflection per fringe

Differential measurement!

Bragg Grating Fiber Optic Strain Gauges

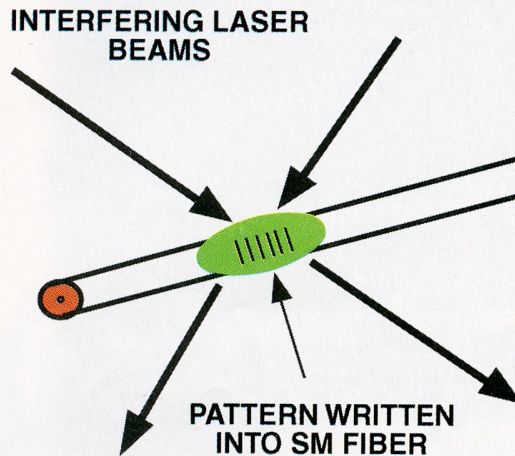


Figure 9. It's possible to write a diffraction grating into the core of a single-mode fiber. The most common fabrication procedure for such gratings involves generating a high-energy, light-dark diffraction pattern using laser(s) whose output wavelength corresponds to an absorption band of the germanium-doped single-mode fiber. The pattern essentially damages the core by locally changing the index of refraction in the high-intensity dark band of the fiber. The spacing between the pattern's dark (or light) bands is called the grating period.

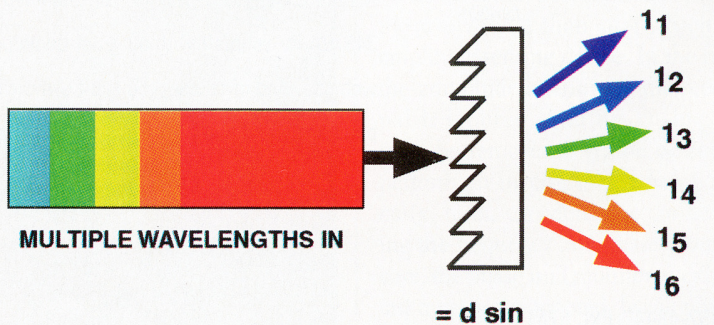


Figure 8. Diffraction gratings, like prisms, force light of different colors to be directed into different angles. Alternatively, if light of different colors enters the grating at the correct angles, all the colors will emerge from the grating traveling in the same direction. This provides an easy and passive method of combining/splitting wavelengths.

Can use PSD with grating for readout (above)
 Or a resonant source (laser) and interfere with a reference
 Can WFDM - code different parts of the fiber to different wavelengths

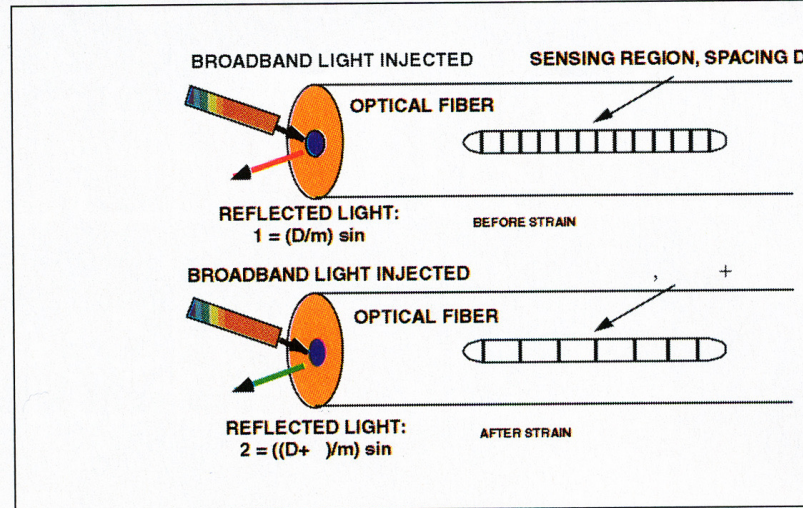


Figure 10. Strain sensing using fiber-optic Bragg gratings may be thought of as analogous to playing an accordian. In an accordian, the tone coming from the instrument changes as it expands and contracts. In the Bragg grating case, the grating was initially fabricated with a certain grating period, which means that when broadband light is injected into the fiber, only a certain wavelength, corresponding to the period, is reflected. When the grating is strained (or stretched like an accordian), the period changes, causing the color of the reflected light to change. Strain sensing happens by monitoring the color of the light being reflected—a color change indicates a certain strain level.

$$m\lambda = d \sin \theta \quad (24)$$

where:

m = an integer (e.g., -3, -2, -1, 0, 1, 2, 3)

λ = wavelength of the light

interacting with the grating

d = physical spacing between the lines of the grating

θ = angle at which the light of wavelength λ will emerge from the grating

Resistive Wire Strain Detection

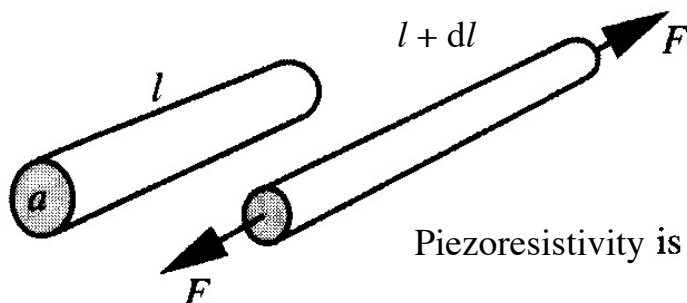


Fig. 3.19. Strain changes the geometry of a conductor and its resistance.

Piezoresistivity is successfully employed in sensors which are responsive to stress, σ :

$$\sigma = \frac{F}{a} = E \frac{dl}{l}, \quad \text{Strain } (e = \frac{dl}{l}) \quad (3.60)$$

where E is Young's modulus of the material and F is the applied force. In this equation, the ratio $dl/l = e$ is called *strain*, which is a normalized deformation of the material.

Figure 3.19 shows a cylindrical conductor (wire) stretched by applied force F . The volume v of the material stays constant while the length increases and the cross sectional area becomes smaller. As a result, Eq. (3.54) can be rewritten as

$$R = \rho(l/a) \longrightarrow R = \frac{\rho}{v} l^2 \quad (3.61)$$

After differentiating, we can define sensitivity of resistance with respect to wire elongation:

$$\frac{dR}{dl} = 2 \frac{\rho}{v} l. \quad (3.62)$$

It follows from this equation that the sensitivity becomes higher for the longer and thinner wires with a high specific resistance. Normalized incremental resistance of the strained wire is a linear function of strain, e , and it can be expressed as

$$\frac{dR}{R} = S_e e, \quad \text{Gauge Factor} \quad (3.63)$$

where S_e is known as the *gauge factor* or *sensitivity* of the strain gauge element. For metallic wires, it ranges from 2 to 6. It is much higher for semiconductor gauges; it is between 40 and 200.

$$R = \rho(l/a)$$

Resistance

Resistivity

Length over cross-sectional area

Strain Gauge Materials

For small variations in resistance not exceeding 2% (which is usually the case), the resistance of a metallic wire is

$$R = R_0(1 + x), \quad (9.5)$$

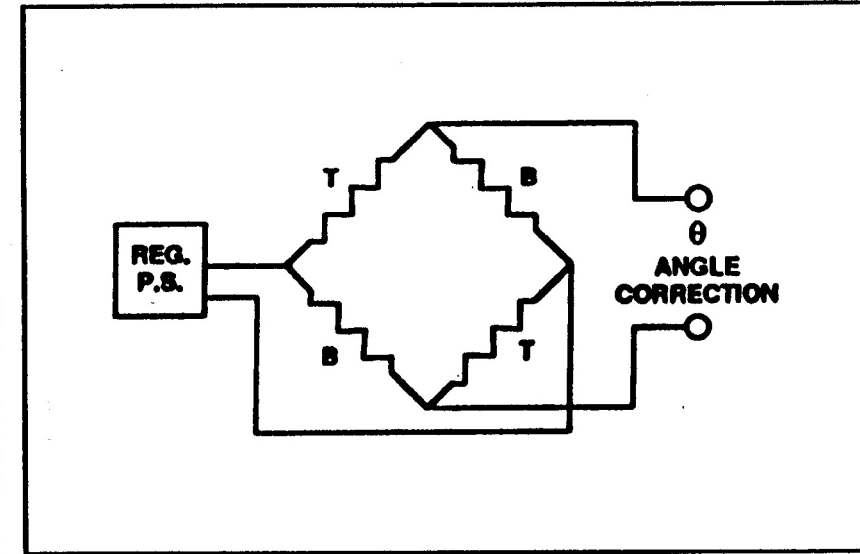
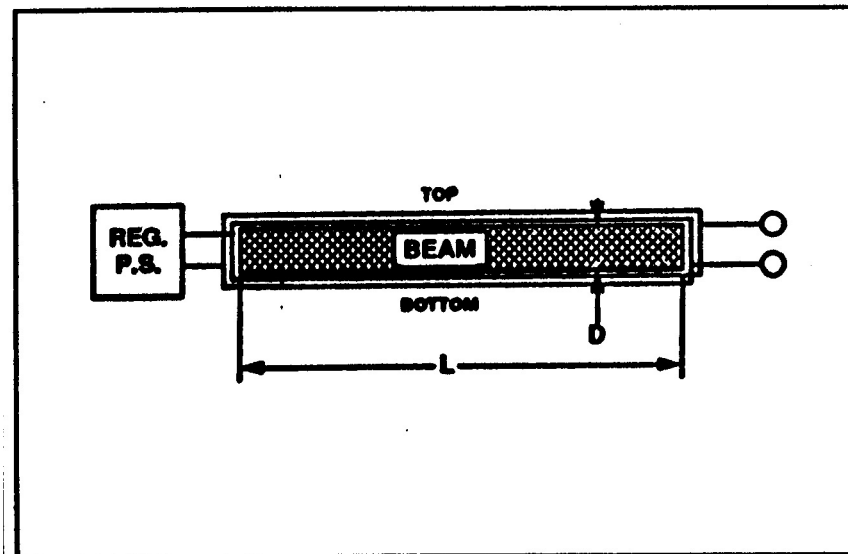
where R_0 is the resistance with no stress applied, and $x = S_e e$. For the semiconductive materials, the relationship depends on the doping concentration (Fig. 18.2A of Chapter 18). Resistance decreases with compression and increases with tension. Characteristics of some resistance strain gauges are given in Table 9.2.

Material	Gauge factor (S_e)	Resistance, Ω	Temperature coefficient of resistance ($^{\circ}\text{C}^{-1} \times 10^{-6}$)	Notes
57% Cu–43%Ni	2.0	100	10.8	S_e is constant over a wide range of strain; for use under 260°C
Platinum alloys	4.0–6.0	50	2,160	For high-temperature use
Silicon	–100 to +150	200	90,000	High sensitivity, good for large strain measurements

Source: Ref. [4].

- Readout strain gauges via a Wheatstone bridge
- Temp. effect: $\rho = \rho_0(1 + \alpha(T - T_0))$
 - Must compensate with backing strain gauge or T measurement

Cheaper AXIS with resistive wire



$$\theta = \frac{\Delta L}{D} = \frac{\Delta L/L}{D/L} \propto \frac{\Delta R/R}{D/L}$$

$$\delta\theta \propto \frac{\delta R/R}{D/L}$$

$\delta R/R$	10^{-6}	10^{-7}
L	6m	6m
D	2cm	2cm
$\delta\theta$	0.30 mrad	0.03 mrad

Axis Results

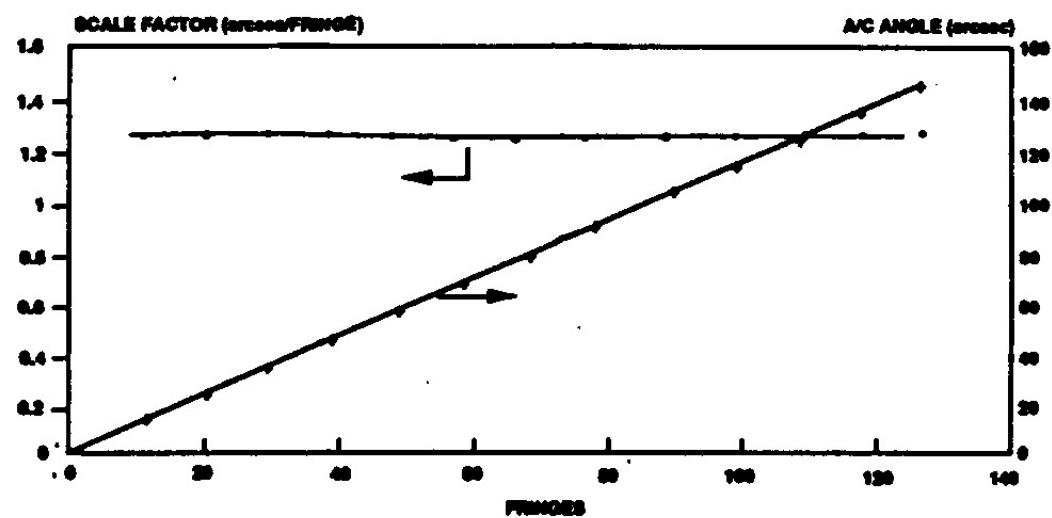
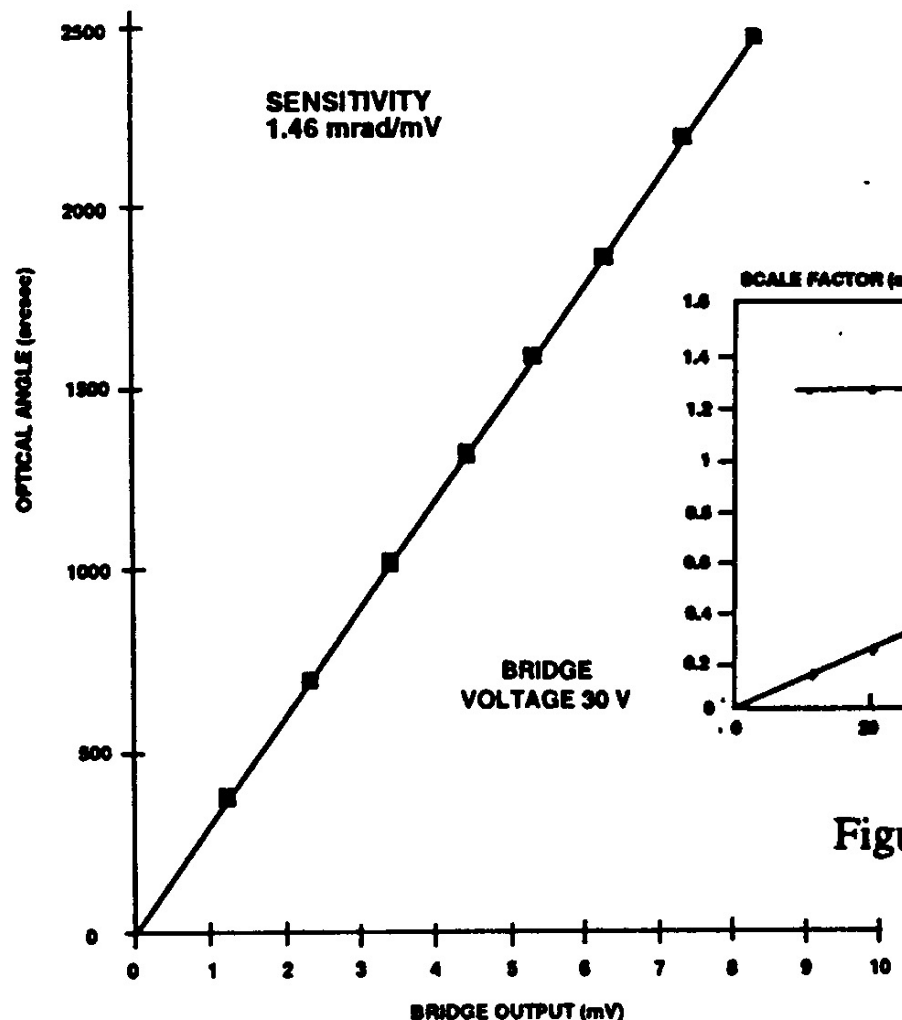


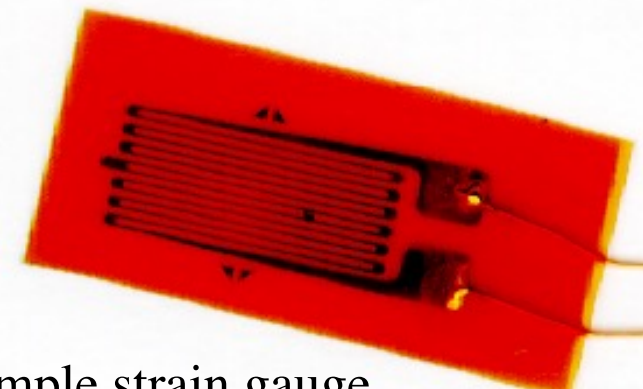
Figure 4. Test Configuration 2 Results.
(Optical Axis)

Figure 6. Resistive AXIS Test Results.

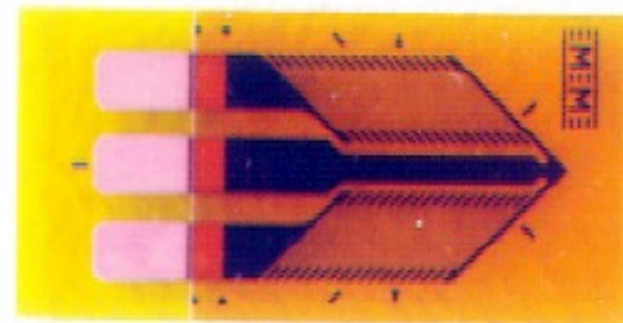
Strain Gauges

A wire strain gauge is composed of a resistor bonded with an elastic carrier (backing). The backing, in turn, is applied to the object for which stress or force should be measured. Obviously, that strain from the object must be reliably coupled to the gauge wire, whereas the wire must be electrically isolated from the object. The coefficient of thermal expansion of the backing should be matched to that of the wire. Many metals can be used to fabricate strain gauges. The most common materials are alloys *constantan*, *nichrome*, *advance*, and *karma*. Typical resistances vary from 100Ω to several thousand ohms. To possess good sensitivity, the sensor should have long longitudinal and short transverse segments (Fig. 9.2), so that transverse sensitivity is no more than a couple of percent of the longitudinal. The gauges may be arranged in many ways to measure strains in different axes. Typically, they are connected into Wheatstone bridge circuits (Section 5.7 of Chapter 5). It should be noted that semiconductive strain gauges are quite sensitive to temperature variations. Therefore, interface circuits or the gauges must contain temperature-compensating networks.

Many manufacturers (e.g., JP Technologies), many patterns...



Simple strain gauge

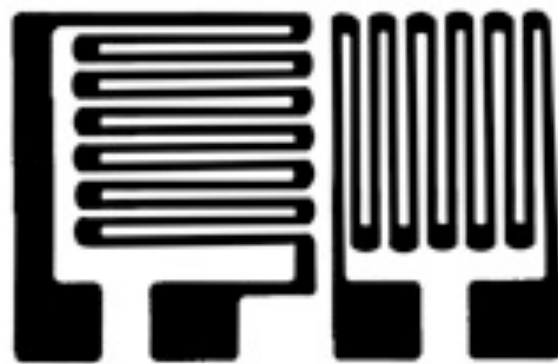


Torsional strain gauge

Strain Gauge Patterns



Linear gauge



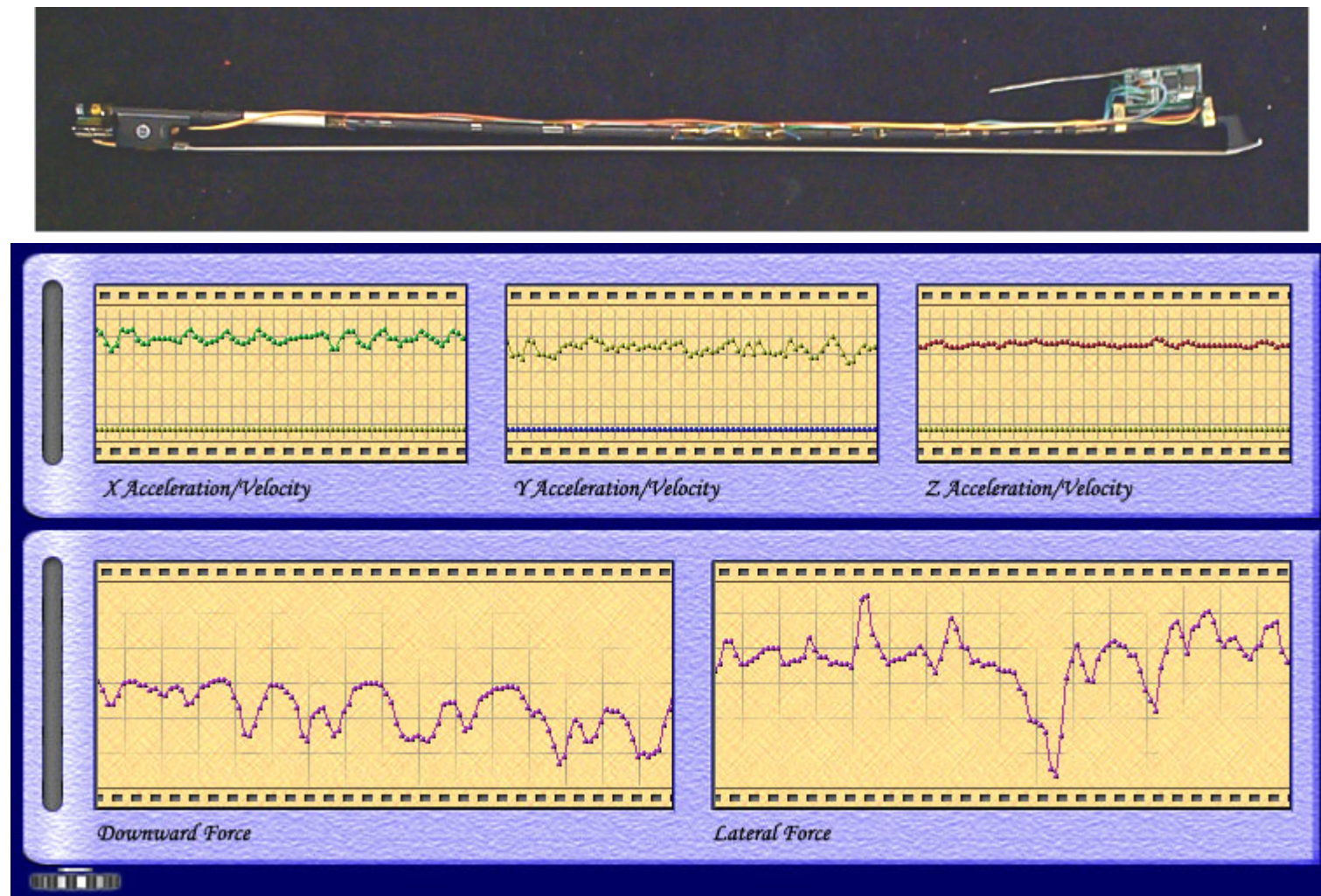
T-rosette



Double shear

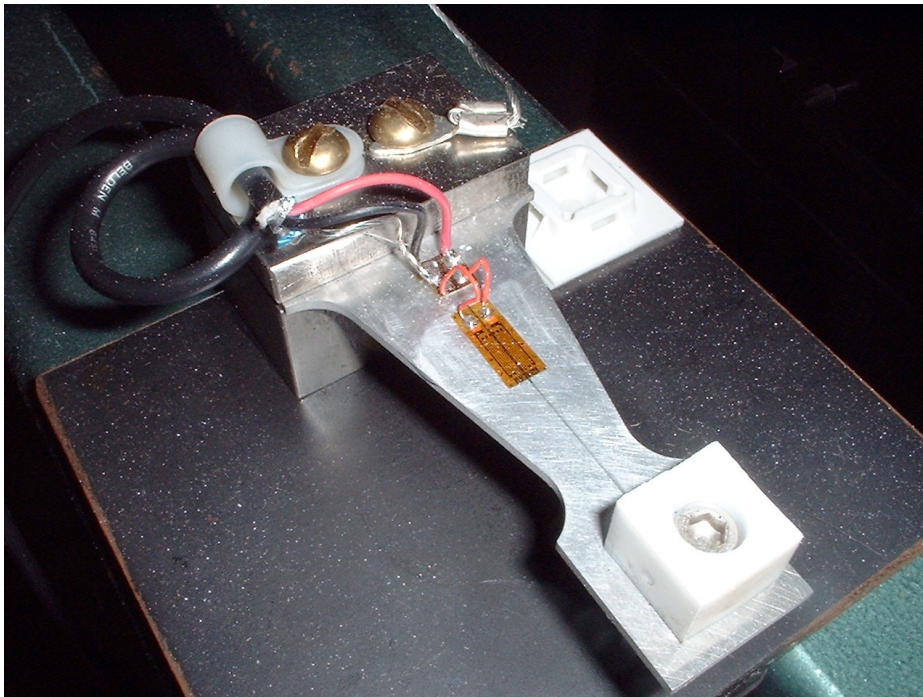
Strain Gauges want to be bonded onto a hard surface, so they can be forced into strain when the surface is deflected. Soft materials won't strain the gauge enough

Current Work – Diana Young's wireless bow



- Strain gauges on bow for bow bend (in x,y) and twist.
- Accelerometers for 3-axis motion
- Capacitive transmitters as before for position

Load Cells



Simple, “naked” load cell from Ohio State

- Bond strain gauge to cantilevered beam
 - Force deflects beam, bends strain gauge, creates signal
- Can be quite accurate
 - Compensate temperature effects



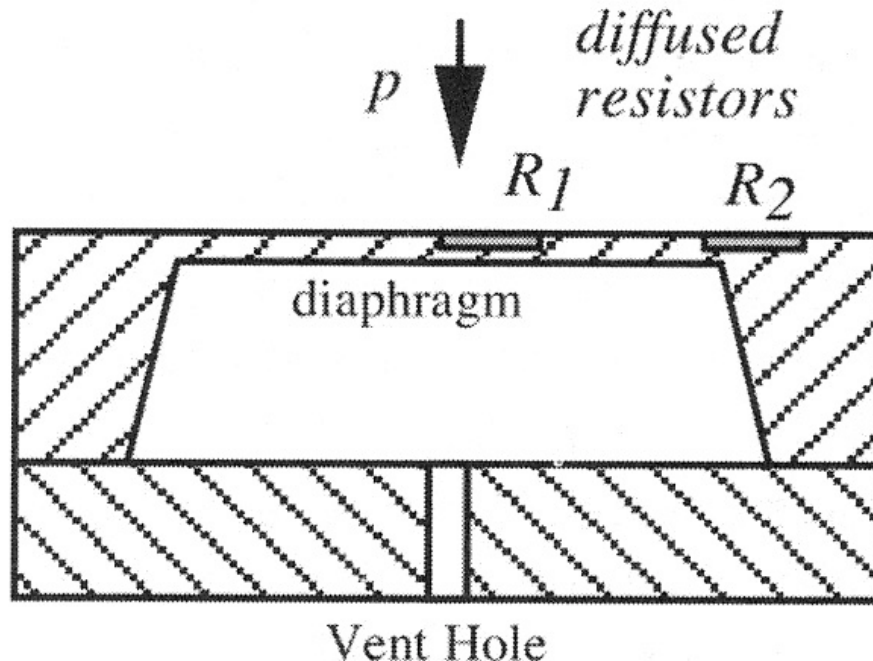
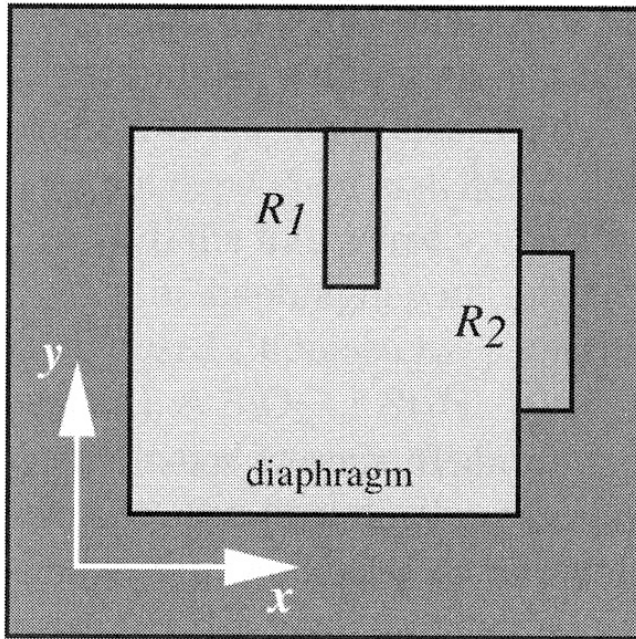
20 Ton load cell for truck weight



Load Cell assortment from DHS

Silicon Pressure Sensors

Fig. 10.4. Position of piezoresistors on a silicon



- Piezoresistors diffused onto silicon at R_1 , R_2
 - Boron doping typical...
- Mechanical stress changes bandgap hence conduction....
- Piezoresistors couple into longitudinal & transverse stress
 - Coupling is opposite for each mode
- R_1 and R_2 essentially subtract in a half-bridge

where π_1 and π_t are the piezoresistive coefficients in the longitudinal and transverse direction, respectively. Stresses in longitudinal and transverse directions are designated σ_1 and σ_t . The π coefficients depend on the orientation of resistors on the silicon crystal. Thus, for p -type diffused resistor arranged in the (110) direction or an n -type silicon square diaphragm with (100) surface orientation as shown in Fig. 10.4, the coefficients are approximately denoted as [7]

$$\pi_1 = -\pi_t = \frac{1}{2}\pi_{44}. \quad (10.11)$$

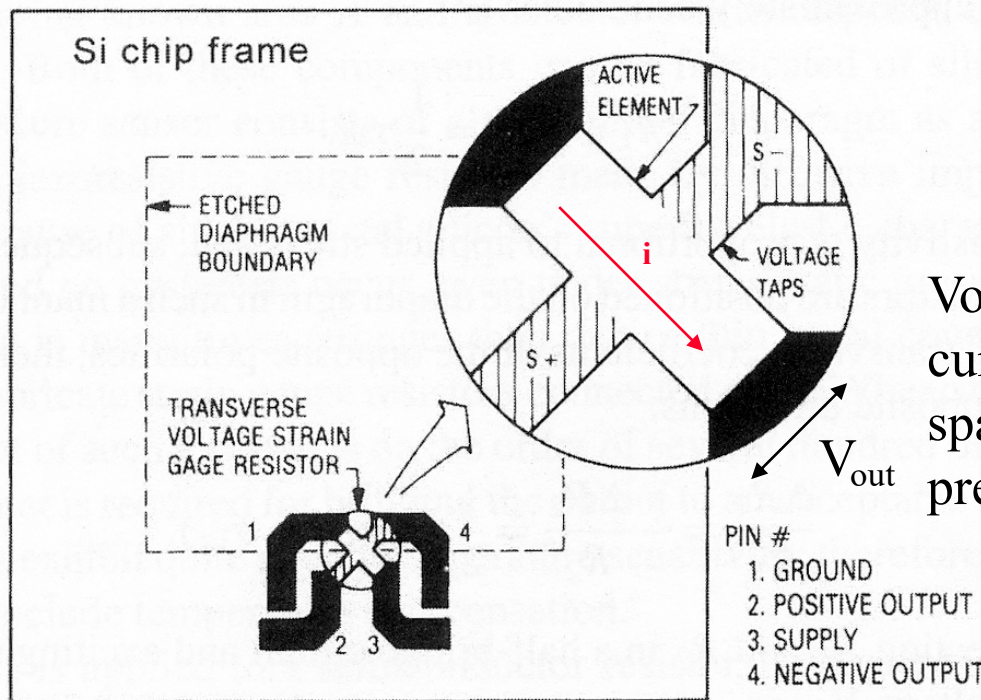
A change in resistivity is proportional to applied stress and, subsequently, to applied pressure. The resistors are positioned on the diaphragm in such a manner as to have the longitudinal and transverse coefficients of the opposite polarities; therefore, resistors change in the opposite directions:

$$\frac{\Delta R_1}{R_1} = -\frac{\Delta R_2}{R_2} = \frac{1}{2}\pi_{44}(\sigma_{1y} - \sigma_{1x}). \quad (10.12)$$

When connecting R_1 and R_2 in a half-bridge circuit and exciting the bridge with E , the output voltage V_{out} is

$$V_{out} = \frac{1}{4}E\pi_{44}(\sigma_{1y} - \sigma_{1x}). \quad (10.13)$$

Motorola MPX Pressure Sensor

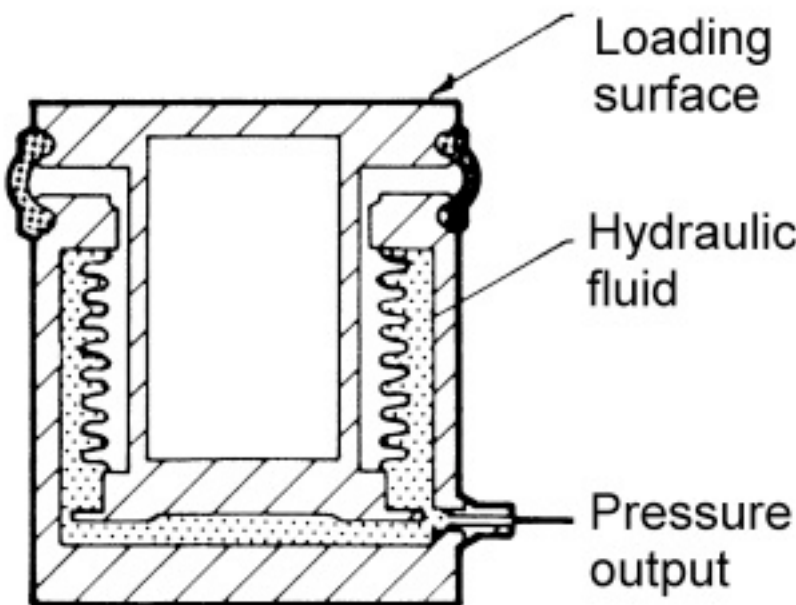


Voltage created when current bends due to spatial R gradient from pressure distribution

Fig. 10.5. Basic uncompensated piezoresistive element of Motorola MPX pressure sensor.
(Copyright Motorola, Inc. Used with permission.)

- Pressure sets up electrical field in non-excited connections (hence voltage)
 - Analogous to Hall effect
 - Essentially already a bridge
 - Everything is on one substrate - simpler T compensation

Pressure Sensors



Hydraulic Load Cell

Link to UW paper on elevators

Many manufacturers: Bosch, Freescale, MSI, Silicon Designs...

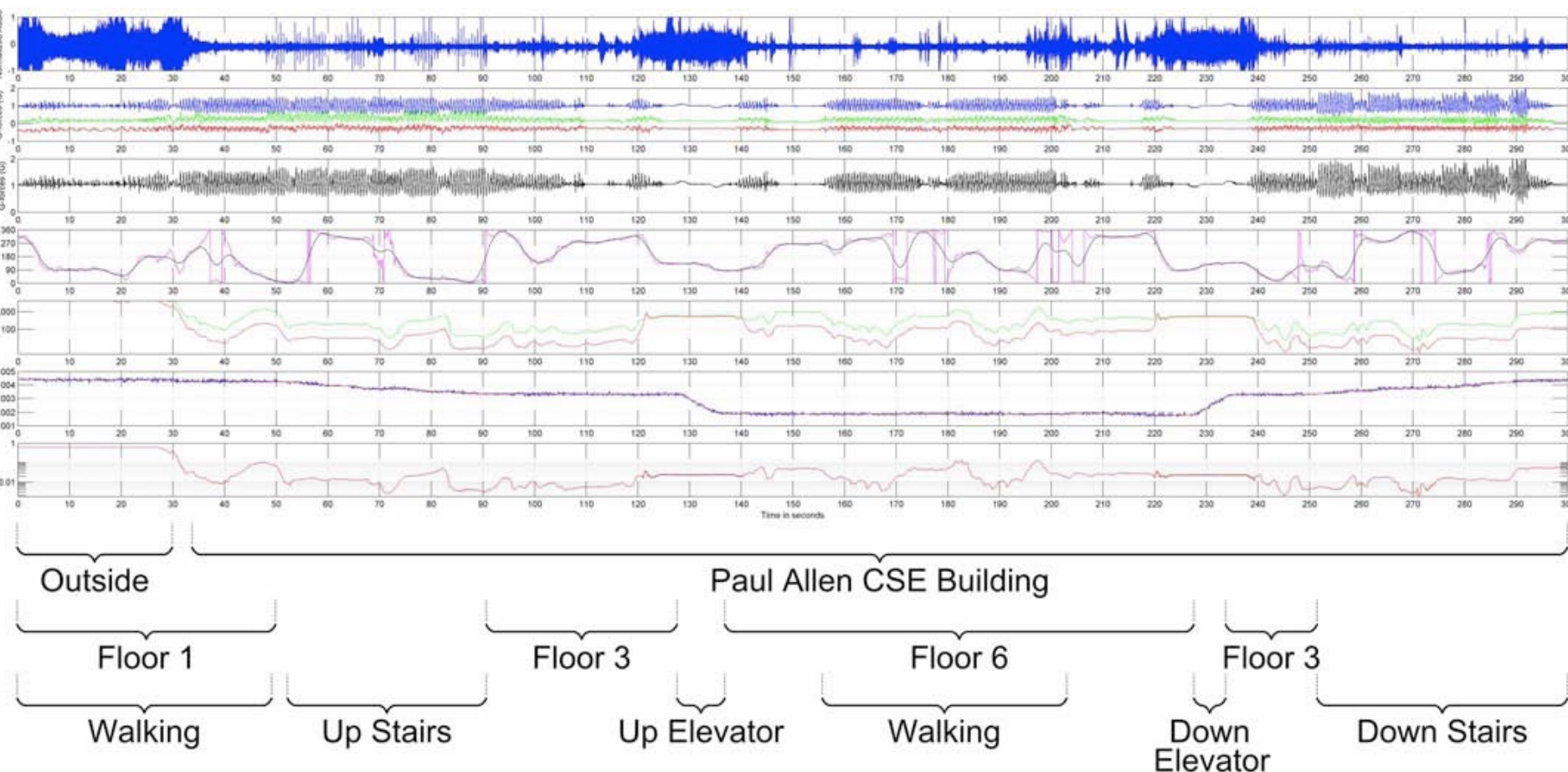
- Absolute and Differential (air or fluid) pressure
 - Back of diaphragm open or closed to the air/medium



MPX 2052D

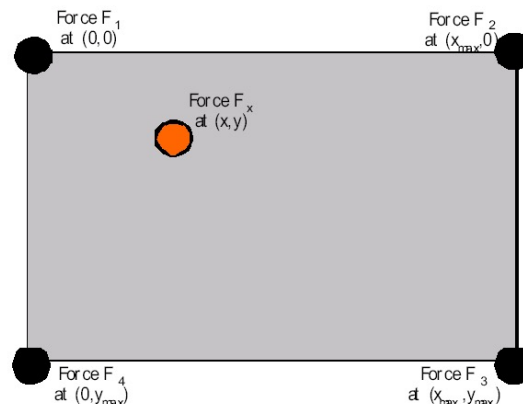


UW/Intel Wearable Monitoring

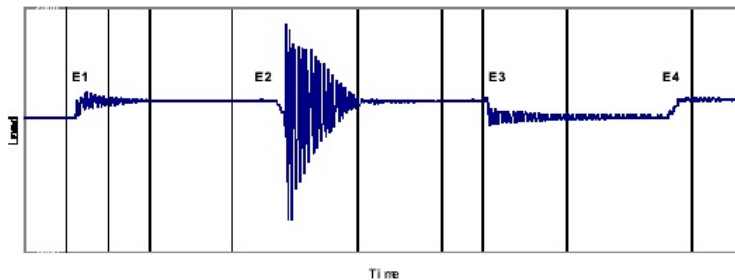


Brunette, W., Lester, J., Rea, A., and Borriello, G. 2005. Some sensor network elements for ubiquitous computing. In Proceedings of the 4th international Symposium on information Processing in Sensor Networks (Los Angeles, California, April 24 - 27, 2005). Information Processing In Sensor Networks. IEEE Press, Piscataway, NJ, 52.

Force Balance Platform



Forces on a surface used to determine the 2 -D position of objects.



By looking at the dynamic pressure balance on the table, objects on the table can be identified by weight change and tracked by force balance. Ditto for people moving around the floor

Albrecht Schmidt, et al., Ubicomp 2002

http://ubicomp.lancs.ac.uk/smart-its/Weight_Table/weight_table.html

$$F_x = F_1 + F_2 + F_3 + F_4$$

$$F0_x = F0_1 + F0_2 + F0_3 + F0_4$$

$$x = x_{\max} \frac{(F_2 - F0_2) + (F_3 - F0_3)}{(F_x - F0_x)}$$

$$y = y_{\max} \frac{(F_3 - F0_3) + (F_4 - F0_4)}{(F_x - F0_x)}$$

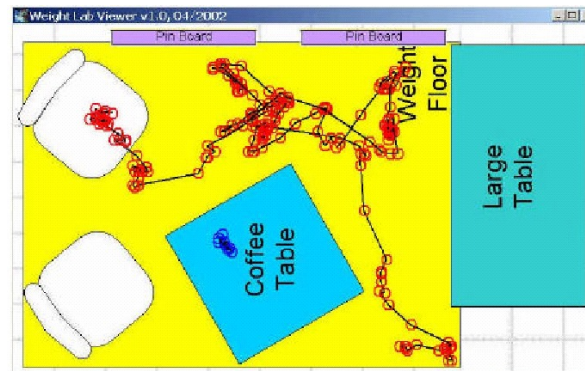
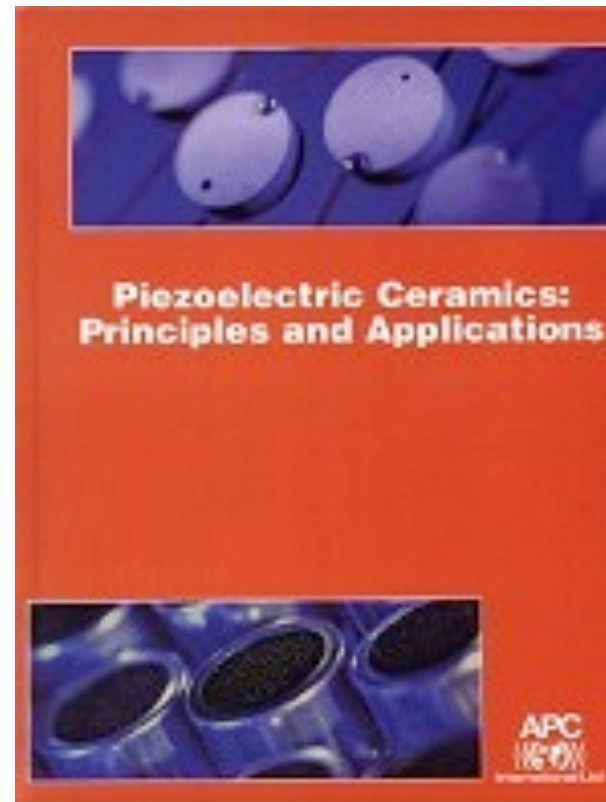


Fig. 8. Weight lab viewer showing a trace on the floor layout of the lab and also some interaction with the table (object put down).



Piezoelectric References



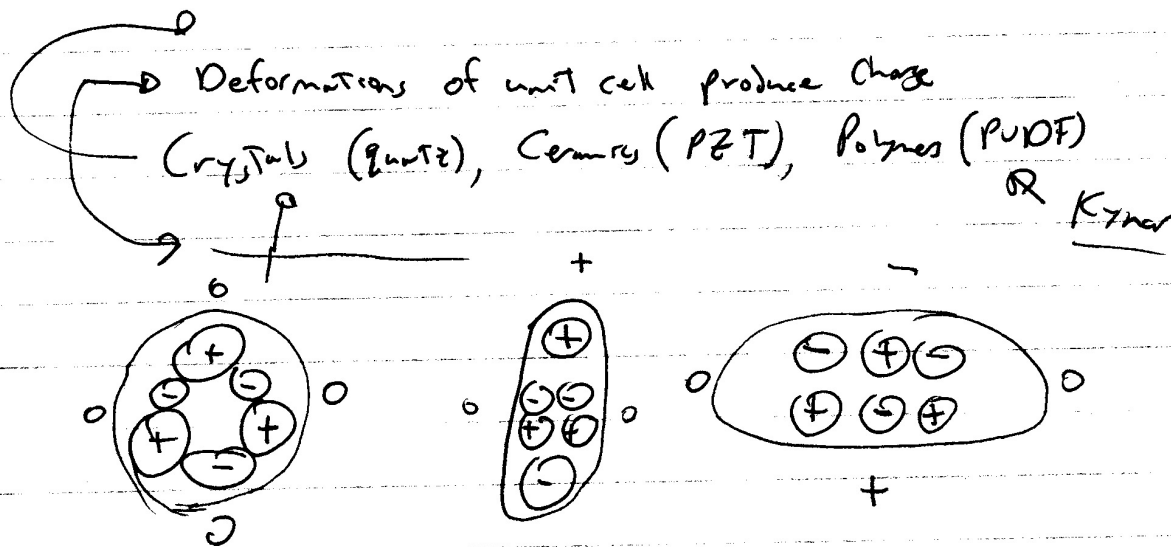
- APC International
 - Piezoelectric Ceramics: Principles & Applications
- Websites:
 - MSI Tutorial, Piezo Systems Tutorial
 - See Class webpage for links and downloads

Piezoelectrics

Piezoelectrics

Measure dynamic force

Ferroelectrics



- Crystal lattice gives intrinsic polarizing

- Ceramics, Polymers need to be polarized

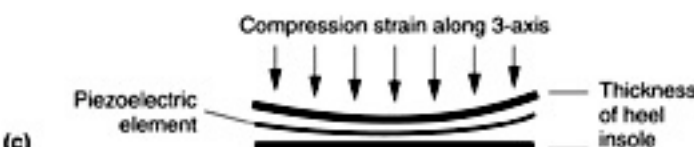
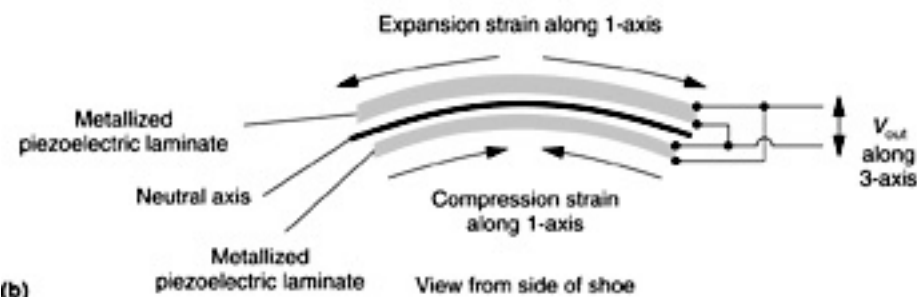
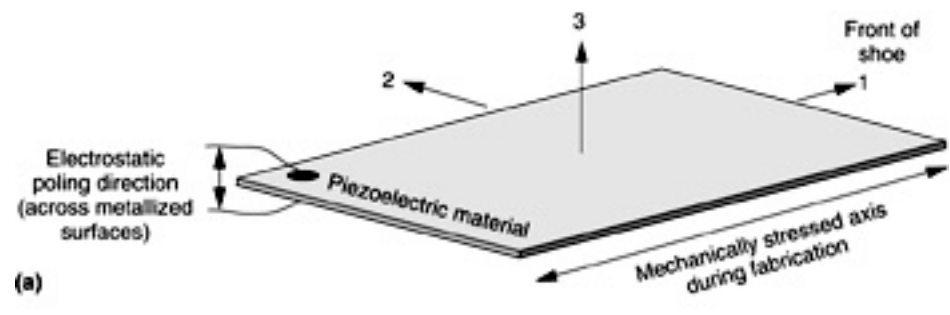
→ \vec{E} field, pulling, Temp (heat) ($>$ cure)

→ Film becomes "semicrystalline homo polymer"

← (+) \vec{F} & \vec{E} axis

Piezo Axes under Strain

Electrodes aluminized, silver inked, carbon (high strain)



Piezo Strain Coefficients:

d_{31}, d_{32}, d_{33} -> Coulombs/Newton (charge/force)

Piezo Voltage Coeficients:

g_{31}, g_{32}, g_{33} -> Electric Field Strength/Pressure
([V/m]/[N/m²])

$$g_{mn} = d_{mn}/\epsilon$$

Pressure <-> Stress

Stress is for solids

Can be in plane too (shear)

Note: Connected here in parallel for power generation

Capacitor - charge collection electrodes along 3 axis

In polling process, material heated, electric field applied along 3, strain along 1

Piezoelectric Coefficients

Piezoelectric materials create electrical charge when mechanically stressed. Among the natural materials with this property are quartz, human skin, and human bone, though the latter two have very low coupling efficiencies. Table 2 shows properties of common industrial piezoelectric materials: polyvinylidene fluoride (PVDF) and lead zirconate titanate (PZT). For convenience, references for data sheets and several advanced treatments of piezoelectricity are included at the end of this chapter [3, 6, 33, 58, 80, 133, 49].

Table 2: Piezoelectric characteristics of PVDF and PZT (adapted from [3, 58, 4]).

Property	Units	PVDF	PZT
Density	$\frac{g}{cm^3}$	1.78	7.6
Relative permittivity	$\frac{\epsilon}{\epsilon_0}$	12	1,700
Elastic modulus	$\frac{10^{10} N}{m}$	0.3	4.9
Piezoelectric constant	$\frac{10^{-12} C}{N}$	$d_{31}=20$ $d_{33}=30$	$d_{31}=180$ $d_{33}=360$
Coupling constant	$\frac{CV}{Nm}$	0.11	$k_{31}=0.35$ $k_{33}=0.69$

PZT $d_{31} = 2.3 \text{ pC/N}$

PZT $d_{31} = 110 \text{ pC/N}$

PVDF: $d_{31} = 23 \text{ pC/N}$, $d_{32} = 3 \text{ pC/N}$, $d_{33} = -33 \text{ pC/N}$

Voltage from Strain

Crystal, Resonant
 bond, resonant
 w. high P

$$D_p = \frac{Q}{A_p} = g_{3n} X_n$$

Charge density
 Charge dens. D
 electric
 stress along n

Freq soft resonance
 Broadband up to GHz

High dynamic range
 (F0:1, 10^{-3} to 10^6 ps)

Stress = Force / Area

3-3 mode

$V = g_{3n} X_n + \frac{F}{w^2}$ Thickness

$V = g_{33} X_n + \frac{F}{R}$ Nearest cm^2

$V = g_{31} X_n + g_{31} \left(\frac{F}{w^2} \right) + g_{31} \left(\frac{F}{w} \right)$

t is small and w is big

Disc

F0:1 core
 P Sheath
 (9-110 mm)
 + wire

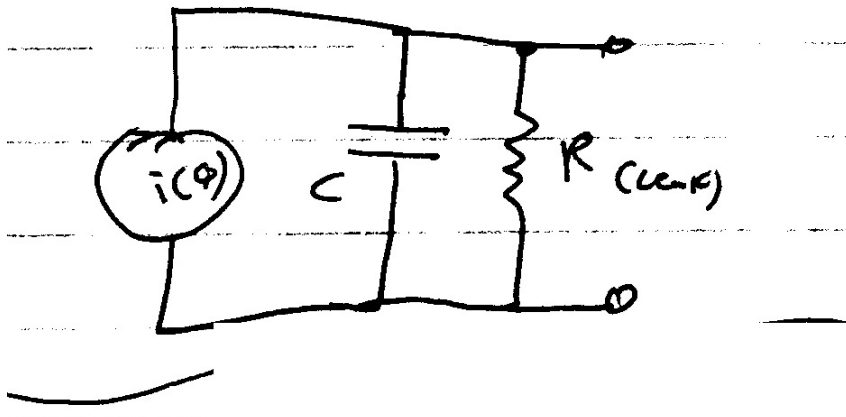
3-1 mode generally much more responsive than 3-3

Piezo Foil (PVDF)

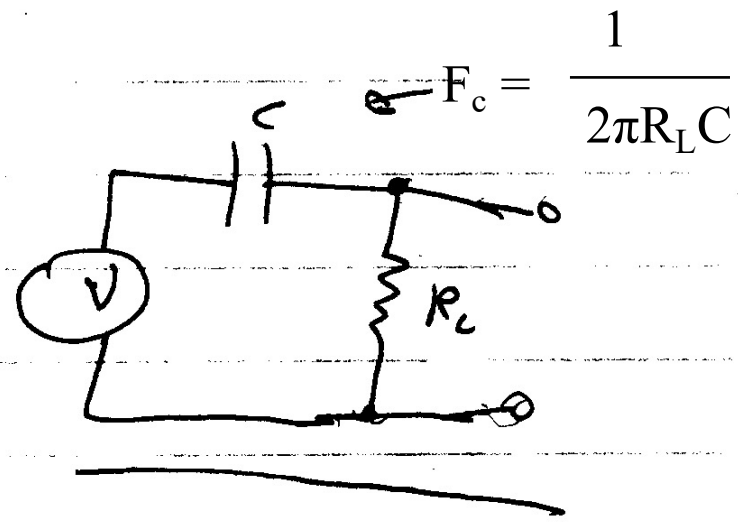


<http://www.meas-spec.com/myMeas/sensors/piezo.asp>

Equivalent Circuits



Charge Model



Voltage Model

High and reactive Impedance!

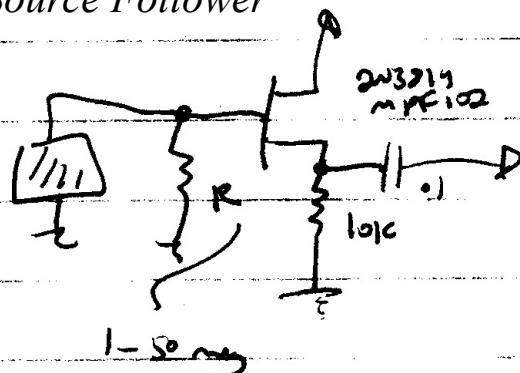
Capacitive Signal Source

Circuits, etc.

Source Follower

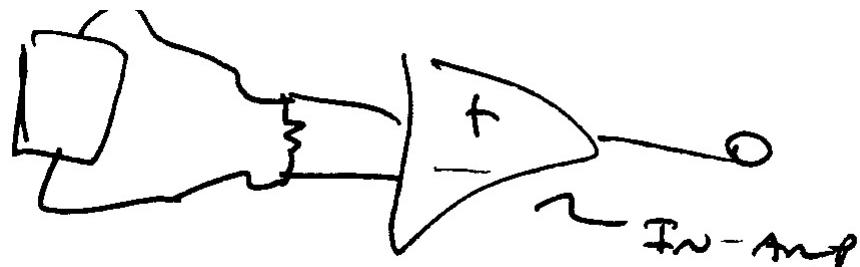
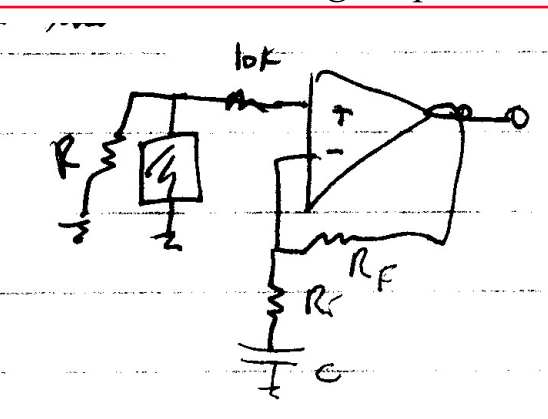
Connecting

pressure
 $\Rightarrow V_{013}$



1-50 mV

Non-Inverting Amp



Some use charge-sensitive (integrating or transimpedance) amplifiers - e.g., to approximate steady-state pressure

I tend to use high-impedance amplifiers for piezoelectric elements

Applications

PVDF uses

→ Rugged, easily interf., nice signals



~ Dynamic Pressure

[Feet, floors, furniture, shoes...]

Morph

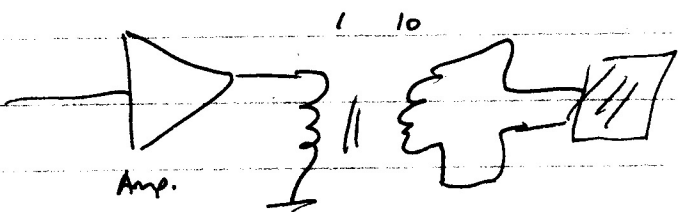
⇒ Acoustic Pick Up [suspension...]

⇒ Sonar

⇒ Distributed Transducer / Array

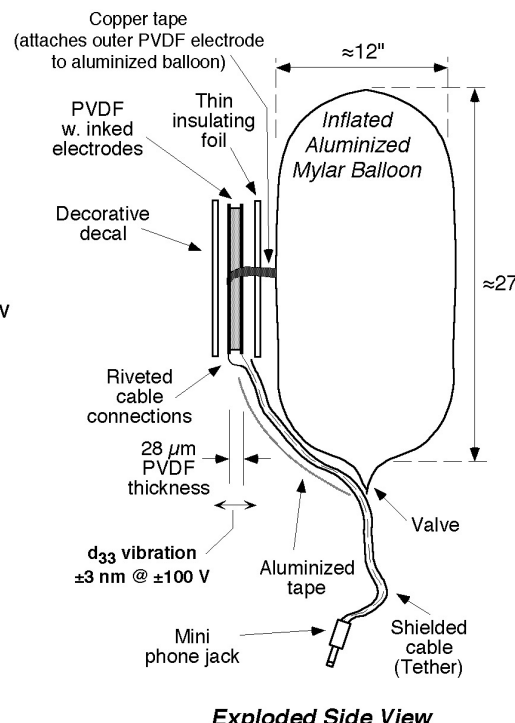
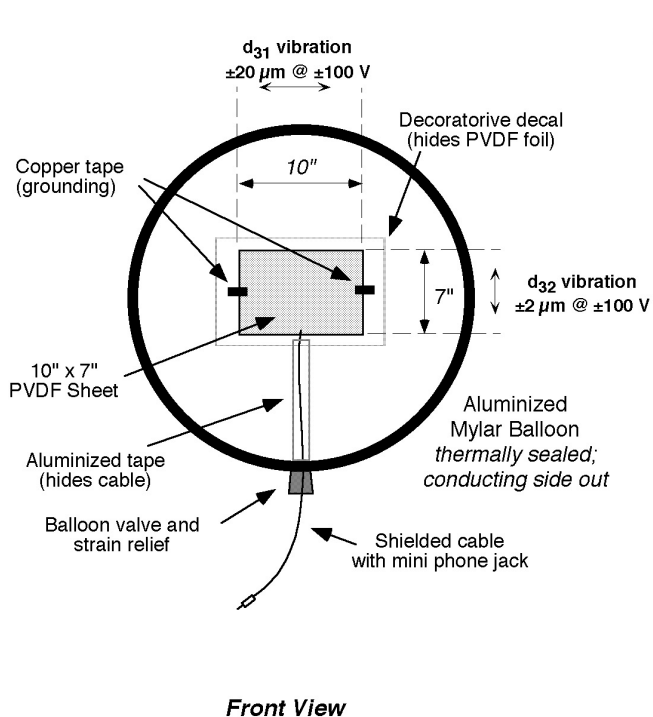
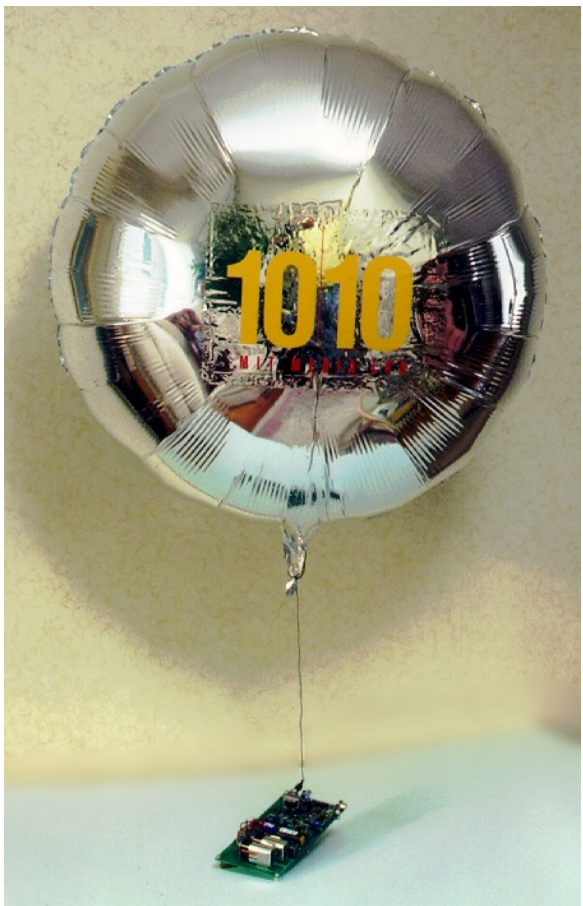
⇒ Reversible ~ Actuator

Thunder



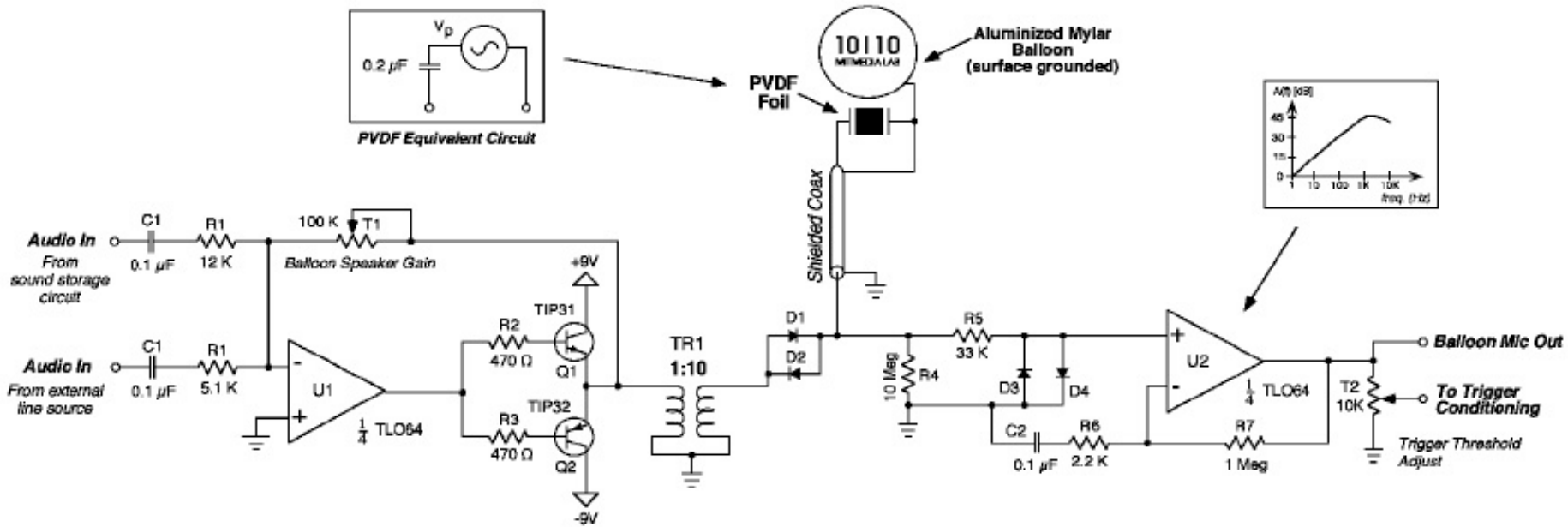
Pa

1995 - Interactive Audio Media



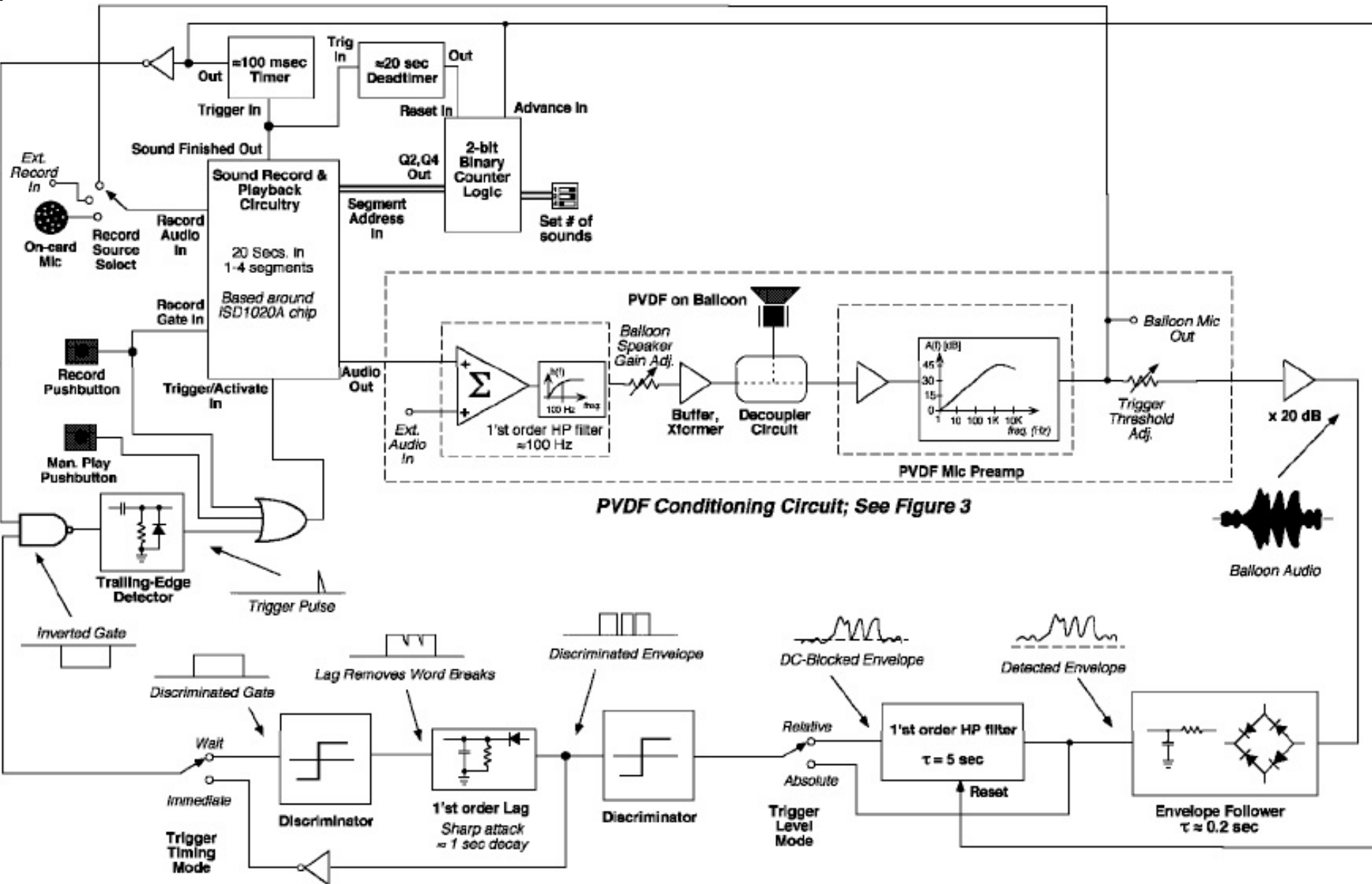
- PVDF strip laminated onto balloon surface forms speaker and microphone
- Simple electronics enable very simple “behavior”
- All over Media Lab for 10'th birthday (60 made)

Balloon Driver/Buffer



Transformer output boost, diode-based TR switch, and HP input response

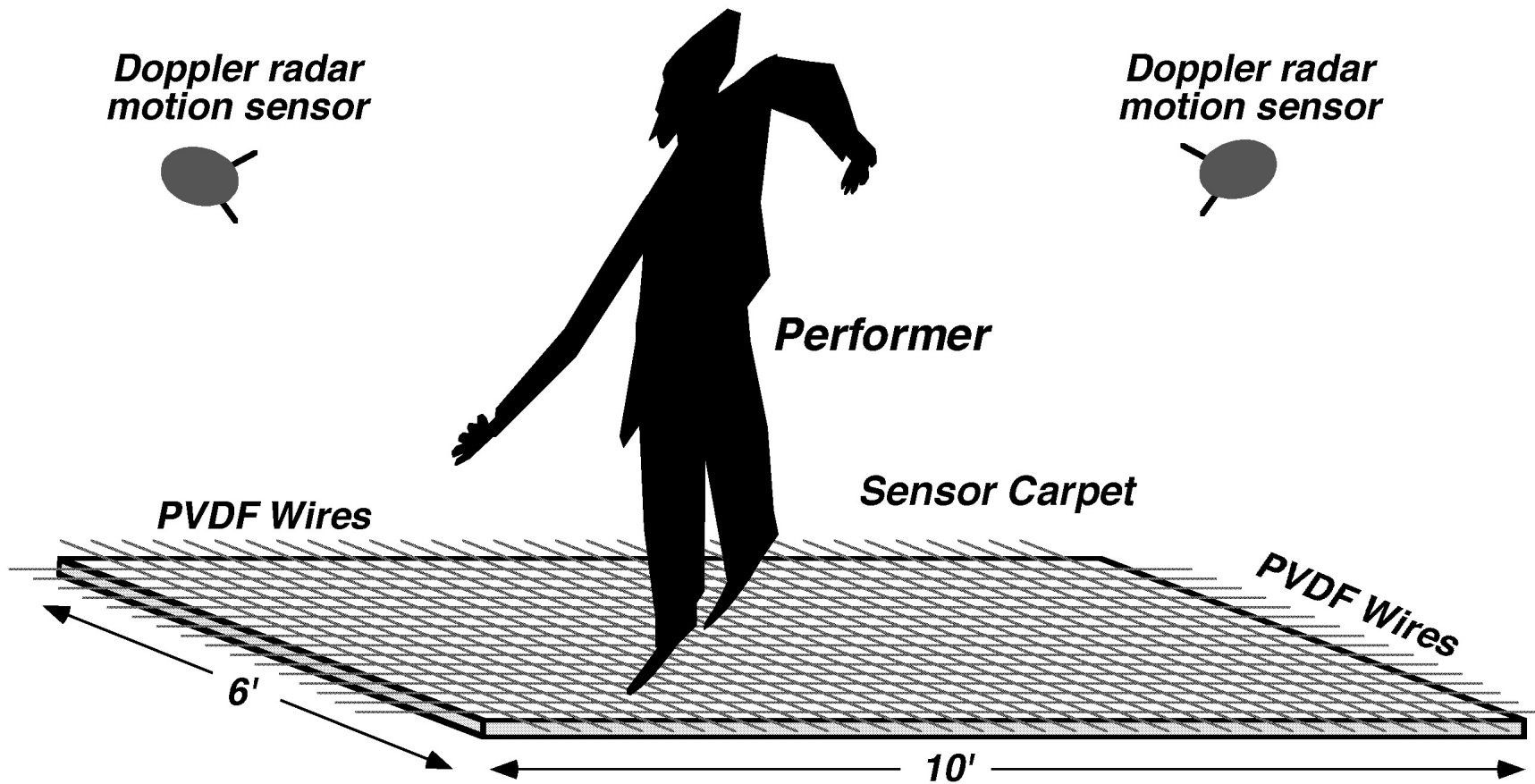
All in Analog(!)



Demo from ~2002

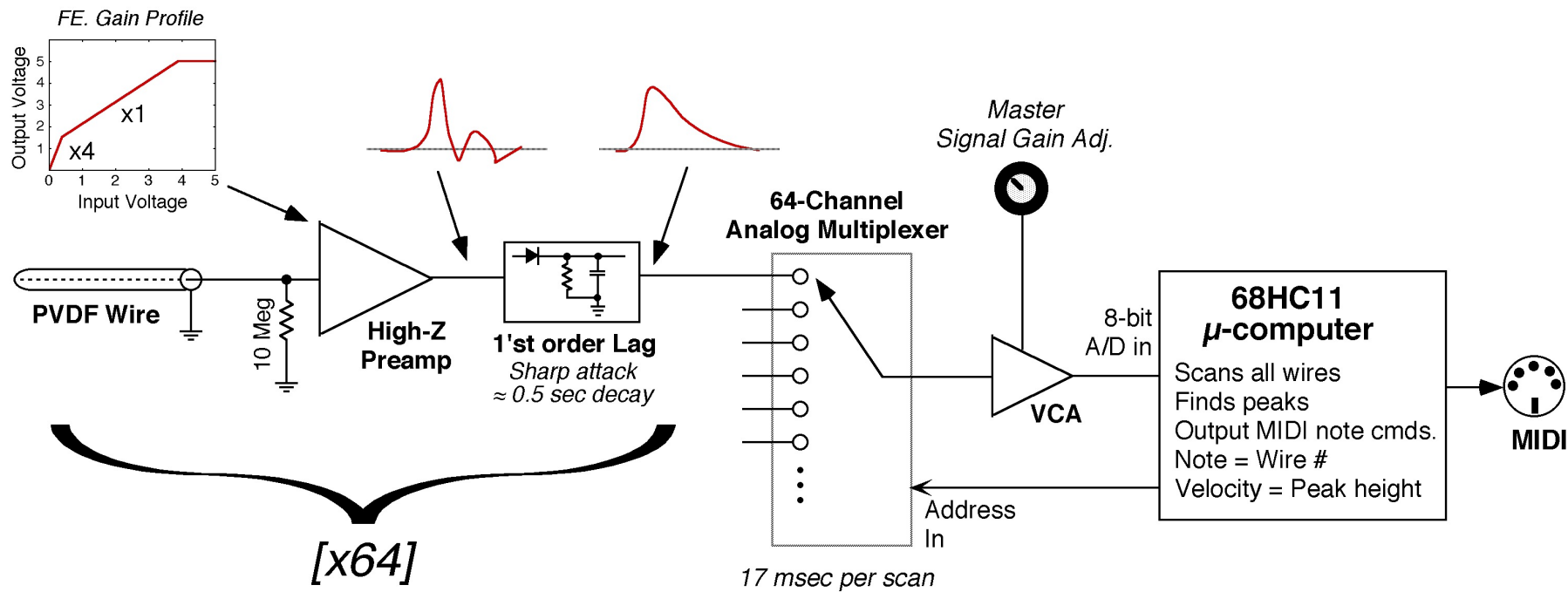


The Magic Carpet



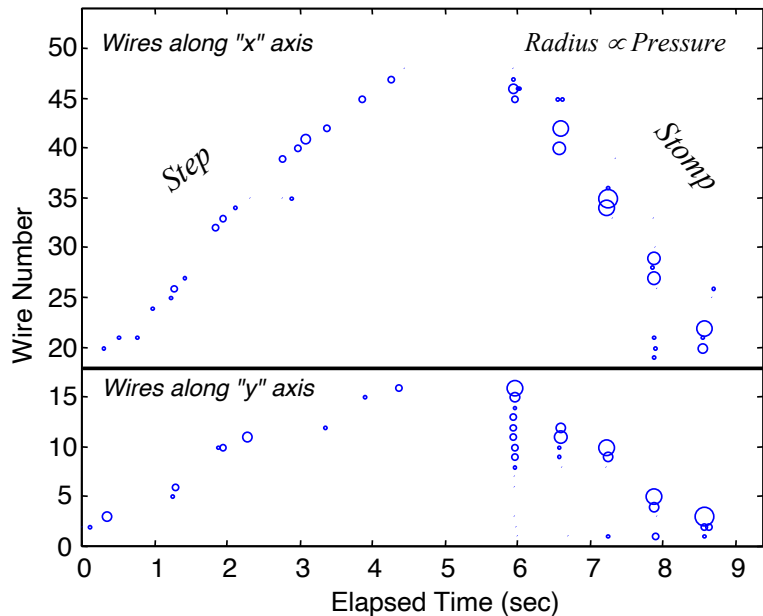
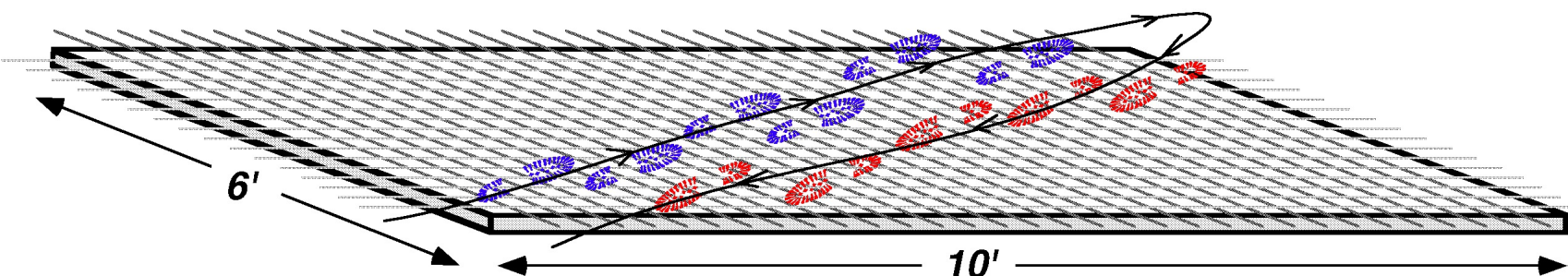
- Foot position, dynamic pressure captured by 4" grid of piezoelectric wire
- Pair of orthogonal Doppler radars measure upper body motion
- Not currently in the Brain Opera...

Sensing in the Carpet

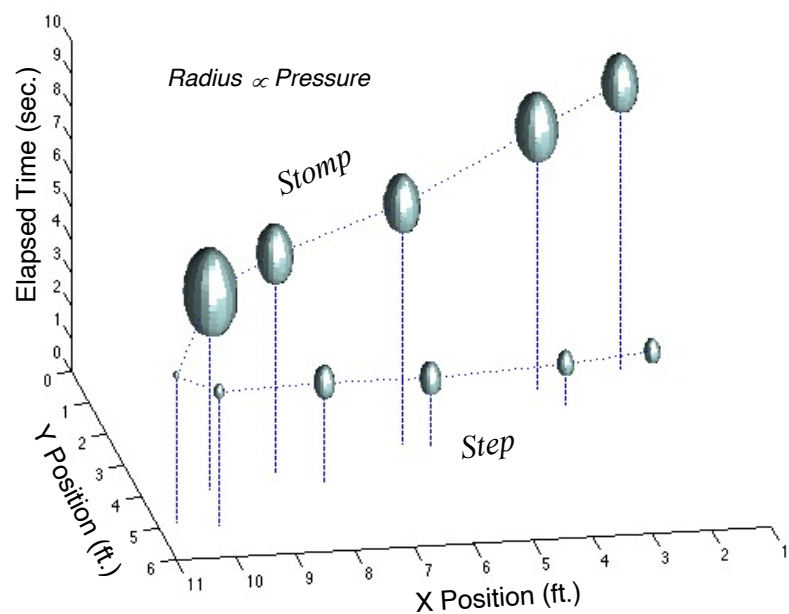


- Up to 64 PVDF wires are sampled at 60 Hz
- MIDI note events generated at every peak
- Simple electronics...

Carpet Data Analysis



Raw data from carpet wires



Data after time clustering

Smart Flooring at the MIT Museum



Stomping Ground

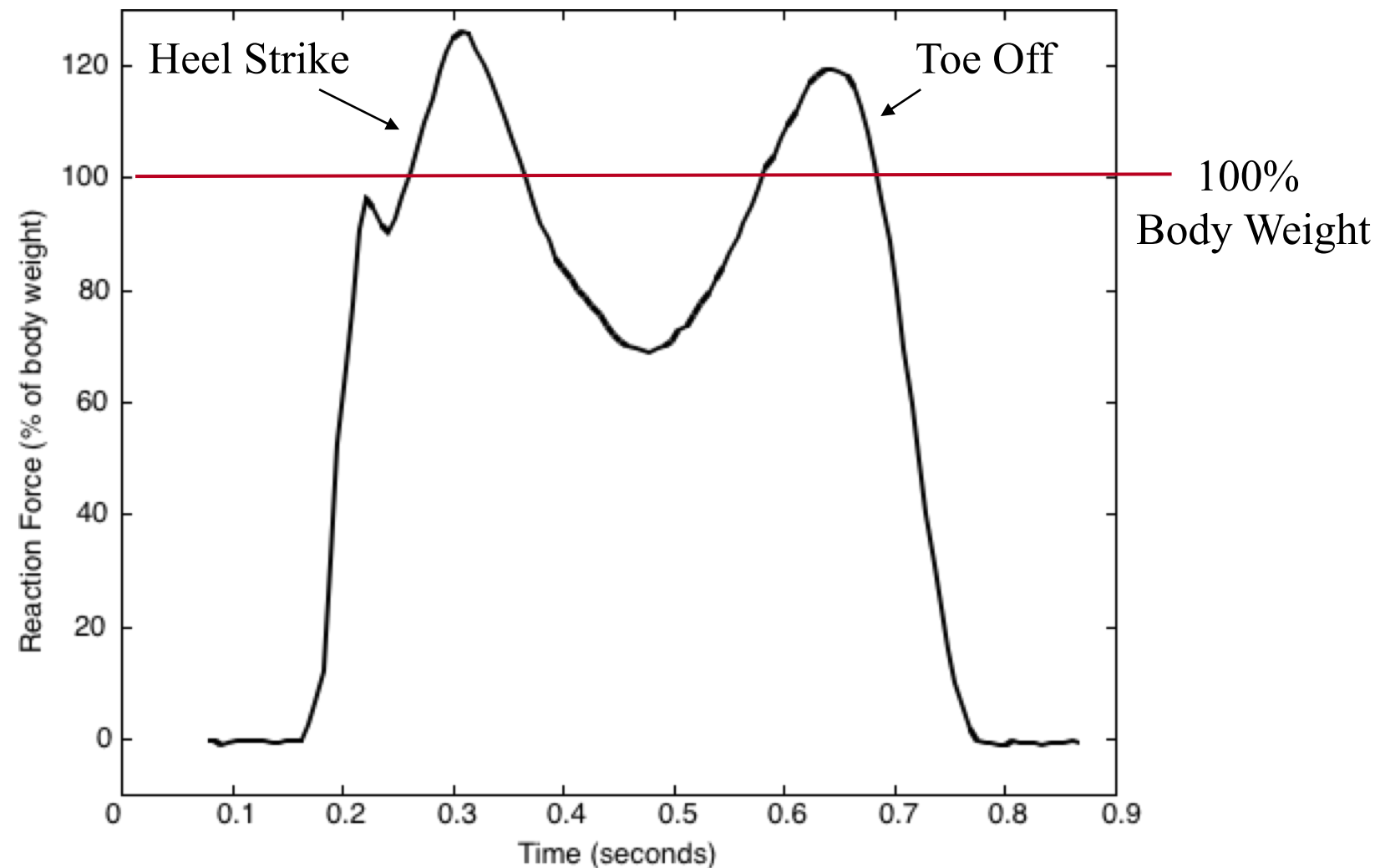
Permanent installation at the MIT Museum, opened 4/30/02

Collaboration with John Maeda's A&C Group (graphics)

First Demo (1998)

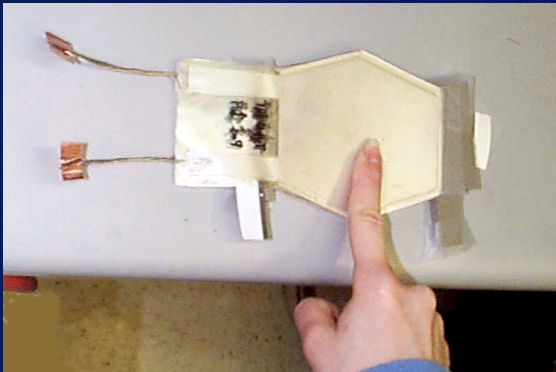


Heel Strike



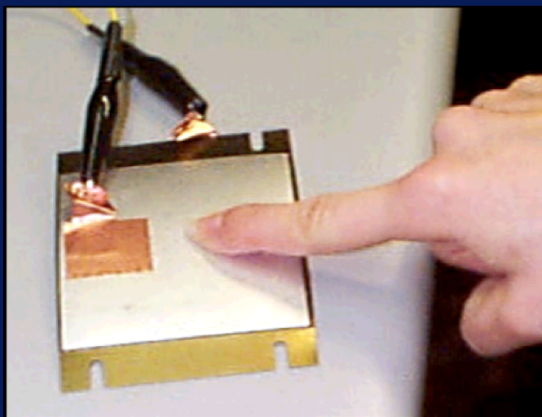
- Force at heel strike and toe off exceeds 100%
 - Heel can compress by 1 cm – Watts possible?

Power Harvesting Insoles - 1998



PVDF Stave
*Molded into sole
Energy from bend*

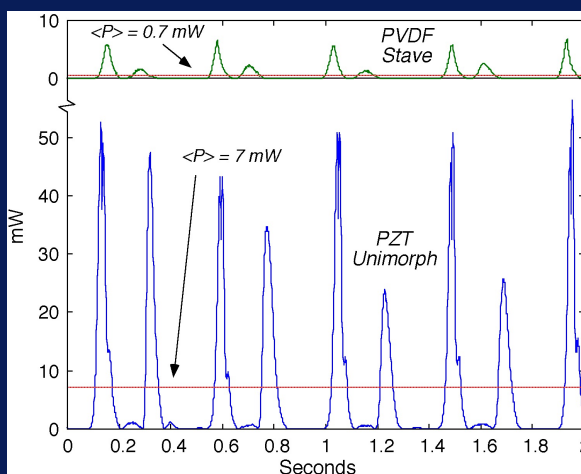
$$P_{\text{peak}} \approx 10 \text{ mW}$$
$$\langle P \rangle \approx 1 \text{ mW}$$



**“Thunder” PZT
Clamshell Unimorph**

*Under insole
Pressed by heel*

$$P_{\text{peak}} \approx 50 \text{ mW}$$
$$\langle P \rangle \approx 10 \text{ mW}$$



**Raw Power
circa 1% efficient
Unnoticeable**

*Responsive Environments Group
MIT Media Lab
1998 IEEE Wearable Computing Conference*

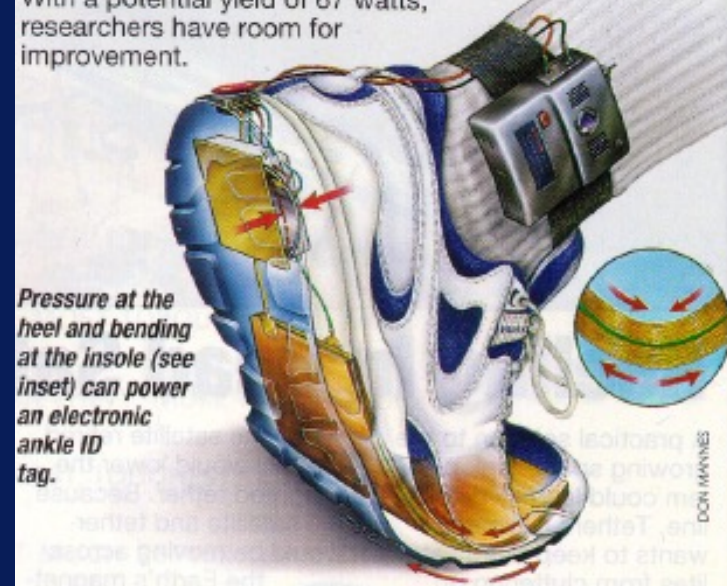
Walking Powers Electronics

High-tech shoes harvesting old-fashioned foot power could someday generate enough electricity for portable phones and computers.

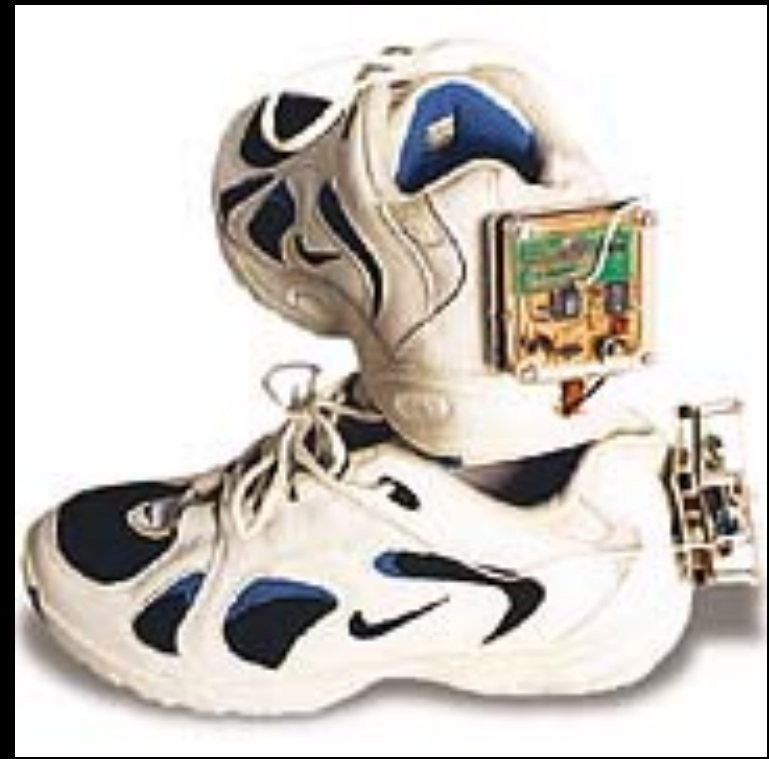
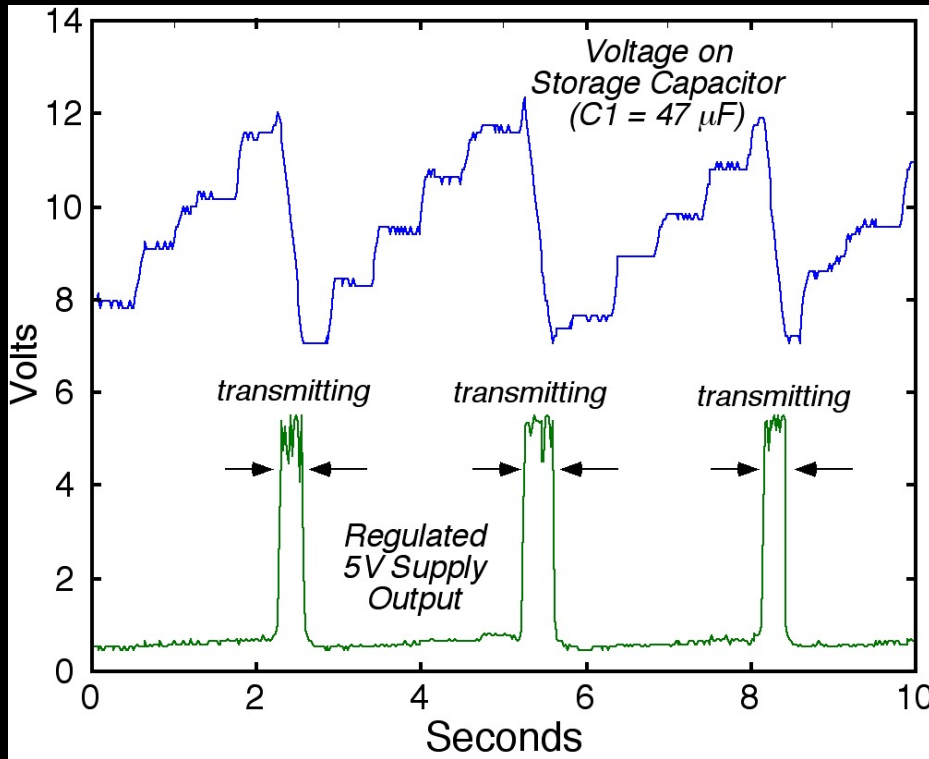
MIT scientists led by Joseph Paradiso, technical director of The Media Laboratory's Things That Work Consortium, have powered simple electronic identification tags with two different devices that resemble cushioned shoe inserts.

Both use the piezoelectric principle by which a physical distortion to a substance produces an electrical potential between its surfaces. One device harvests heel strikes' energy with a stiff piezoceramic material. The other device turns the flex in a sneaker's insole into electric power via a multilayered laminate of piezoelectric foil.

Power is measured in milliwatts. With a potential yield of 67 watts, researchers have room for improvement.



Application: Batteryless RF Tag



- Use Piezo-shoes to charge up capacitor after several steps
- When voltage surpasses 14 volts, activate 5 V regulator
 - Send 12-bit ID 6-7 times with 310 MHz ASK transmitter
- After 3-6 steps, we provide 3 mA for 0.5 sec
 - Capacitor back in charge mode after dropping below output

Passive Hydraulic Chopping to Excite PZT at Resonance



- Antaki, et al., 1995
 - Passive hydraulic resonant excitation of piezoceramic stack during heel compression
 - Big, kludgy shoe
 - Developed to power artificial organs
 - Developed order of 0.2 – 0.7 Watt average power
 - 2 Watts from simulated “jogging”

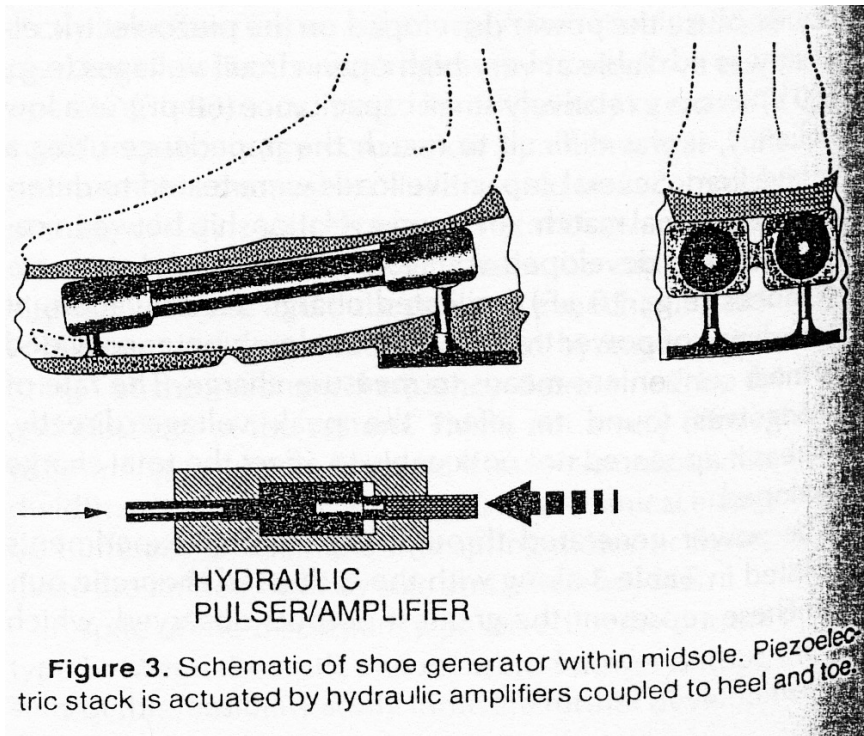
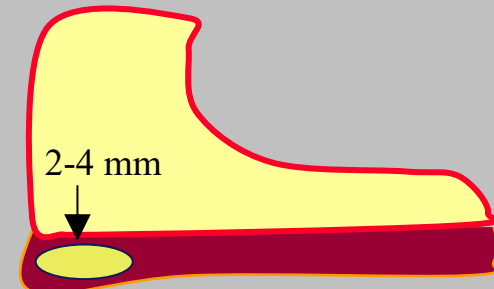
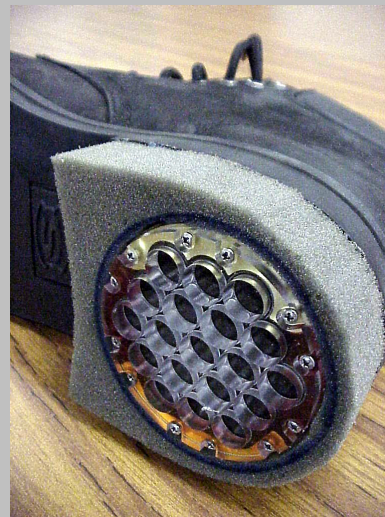
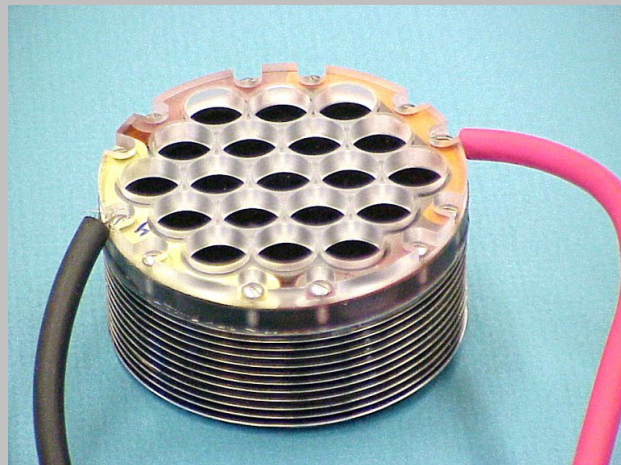


Figure 3. Schematic of shoe generator within midsole. Piezoelectric stack is actuated by hydraulic amplifiers coupled to heel and toe.

Electro-active Polymers under the heel



- Electrostatic generator with silicone rubber or flex acrylic elastomer between the plates
 - Placed under heel
 - 2-4 mm of squeeze gives 50-100% area strain
 - 4 kV across them!
 - Saw 0.8 Watt per shoe (2 Hz pace, 3 mm deflection)
 - Estimate that 1 Watt is possible with more deflection

Ron Peltine, Roy Kornbluh - SRI International